# UNDERSTANDING THE EFFECT OF AMIDE AND AMINE GROUPS ON THE STRUCTURAL AND THERMAL PROPERTIES OF BIOMATERIALS AS A FUNCTION OF IONIC LIQUIDS

By

AMNAH HADADI

A thesis submitted to the

Graduate School-Camden

Rutgers, The State University of New Jersey

In partial fulfillment of the requirements

For the degree of Master of Science

Graduate Program in Chemistry

Written under the direction of

Dr. David Salas-de la Cruz

and approved by

_____

Dr. David Salas-de La Cruz

_____

Dr. Alex J. Roche

_____

Dr. Luca Larini

Camden, New Jersey

May 2017

THESIS ABSTRACT

Understanding the effect of amide and amine groups on the structural and thermal properties of biomaterials as a function of ionic liquids

By

AMNAH HADADI

Thesis Director:

Dr. David Salas-de La Cruz

The blending of macromolecules such as proteins with polysaccharides has many applications in the medical and environmental sectors, such as scaffolding for tissue engineering and as water filtration membranes for the removal of heavy metals. However, our inability to predict the relationship between molecular interactions and spatiotemporal structures is preventing their rapid utilization and commercialization. Up-to-date, we have learned the importance of appropriate hierarchical and secondary structures upon material dissolution and regeneration, and its effect on the physicochemical properties. However, much more knowledge is required to fully understand molecular self-assembly behavior and spatiotemporal morphology in blended systems to attempt to define and characterize the basic phenomenon and mechanisms to control the cell-biomaterial interactions or remediation efficiencies. In this work, we focused on understanding the association behavior of protein in the presence of polysaccharide and the effect of acetamido and amine groups on the structure with the utilization of ionic liquid solvents. In the first study, the ionic liquid 1-allyl-3-

methylimidazolium chloride (AMIMCl) was used to dissolve individual polysaccharides (e.g. cellulose, chitin, and chitosan) with protein (e.g. silk). Water is used as the coagulating agent. The upper and lower proportions of silk were used to test the crystallinity of the beta sheet and to understand how the functional groups of each polysaccharide may interact differentially with increasing silk concentrations. The various blended polymers were characterized using Attenuated Total Reflectance Fourier Transform Infrared spectroscopy (ATR-FTIR), Thermogravimetric Analysis (TGA), Differential Scanning Calorimetry (DSC) and Scanning Electron Microscope (SEM) techniques. The results showed that increasing the silk content in the polysaccharides can increase the molecular interactions between the biopolymers, causing an increase in the stability of the blended film; especially, the formation of beta sheets. The second study investigated the effects of different ionic liquids 1-allyl-3-methylimidazoliumchloride (AMIMCl), 1-ethyl-3-methylimidazoliumchloride (EMIMCl) and 1-ethyl-3-methylimidazolium acetate (EMIMAc) on the structural modification, thermal stability and topology of blended films comprised of chitin with silk. Similarly, the third study investigated the effect of AMIMCl and EMIMCl on the structural changes and thermal properties of blended film comprised of chitosan with silk. We observed the modification of the structural, morphological, and thermal properties according to their variances in anion and cation species of the ionic liquid, as well as the silk composition. We notice that the size and the number of interaction sites of the anion can play a role in thermal stability. The increase of the silk content promotes the increase of the crystallinity of the beta sheet in all prepared films.

## Dedication

I would like to dedicate this work to my husband Mater, for his support and for being beside me in my educational studies, to my beautiful daughters Wasan and Wesal, and to my handsome son Fahad. I also dedicate this to my mother Aisha, my father Zain, and my sisters and brothers for their invocation prayers, support and motivation. Also, I dedicate my study in the United States to King Abdul-Allah (May God have mercy on him) who granted Saudi students an opportunity to study abroad with all costs paid and academic monitoring under the name of Saudi Arabian Culture Mission (SACM).

**Acknowledgements**

I would like to thank my adviser Dr. David Salas-de la Cruz for granting me an opportunity to do my master thesis in his lab. Also, I thank him for his advice, support, and patience. I would like to thank Dr. Alex J. Roche and Dr. Luca Larini for being part of my committee. Also, I would like to thank Dr. Georgia Arbuckle-Keil who is the greatest graduate director. Furthermore, I would like to thank Dr. Salas' lab team (John Stanton, Ashley Lewis, Laura Malek, Darrel Cowan, Dalia Alshahrani, Prabhdeep Pandher, Tyler Brown and Stacy Walsh) for their collaboration and help. I would like to thank my friend Asma who had a hand to grab me here and Kate Slobodenko who is the lab technician for her quick assistance any time I needed her. Finally, I would like to thank everyone I met at Rutgers-Camden who helped me during my study.

## Table of Contents

# Chapter 1: Introduction

## Biomaterials

Biomaterials science is the study of the natural-based materials that is used for a medical, environmental or energy application. It is an attractive field of science showing a strong growth over the last fifty years, stimulated by advances in cell and molecular biology, chemistry, material science, and engineering [1, 2]. For example, biomaterials can be used to make devices to replace part of a living system without causing a harmful tissue reaction or a systemic toxic reaction. Biomaterials are categorized into two main groups: natural and synthetic materials. Standard examples of synthetic materials used in biomedical treatment include metal hip replacements and Dacron [3]. Despite the fact that both natural and synthetic materials have been broadly used in medicine, in cancer research and anti-inflammatory therapies and tissue engineering applications [4, 5], natural biomaterials are still preferred due to their unique biocompatibility properties. Indications of biocompatibility include acceptance by the host tissue and/or the whole body, biodegradability, nontoxicity and tuning ability [1, 3, 6].

Natural biomaterial includes numerous materials that are mainly produced by plants and animals such as proteins and polysaccharides. Humans widely have relied on natural materials throughout history. There is great interest of natural materials research due to increasing demand of environmental protection, along with limitations of the petroleum reserves. Thus, biopolymers are the best suitable candidates in this field. Along with its advantages, the increase use of biopolymers leads to the development of chemical and biochemical research to obtain and modify the natural polymer used in a wide range of utilities [7].

**Polysaccharides**

Among natural polymers, polysaccharides are polymeric carbohydrates molecules that have many diverse biomedical applications due to their accessibility and biocompatibility [8]. Approximately 75% of the organic materials in nature are present in the form of polysaccharides [6]. Polysaccharides consist of long chain monosaccharide units linked together by glycosidic bonds. Most of these polysaccharides are considered to have medium to high in molecular weight. They differ from each other by the repeating units, length of their chains, types of bonds linking the monomers and the degree of branching [9]. When all monosaccharides are the same type of monomeric species, it is called a homopolysaccharide or homoglycan; while the presence of different monomeric species within a polysaccharide is considered a heteropolysaccharide or heteroglycan. In general, polysaccharides are important building blocks used in biological systems such as the storage of nutrients in the form of starch or glycogen or as structure elements such as in plant cell walls as cellulose and chitin. Extracted and modified polysaccharides are utilized in various applications of food, chemical, energy production, and pharmaceutical industries [10]. By far, polysaccharides have shown to be antitumoral and to have antiviral activity, as well as the potential for use in the diagnosis and prevention of bacterial infections [11]. Although cellulose, chitin and chitosan are homopolysaccharides that share the same type of (β1-4) glycosidic bond connected by repeating units, they have different mechanical and physical properties.

**Cellulose**

Cellulose is a linear homopolysaccharide found in the cell wall of plants, constitutes much of the mass of wood and cotton and is the most abundant natural polymer on earth [9, 12]. It is also present in many different living organisms such as algae, fungi, bacteria and some sea animals such as tunicates [13]. Its molecular weight depends on its sources as well as the extraction conditions for the purification. In addition, cellulose is a fibrous, tough, water insoluble polymer composed of (β1-4) D-glucose units; it is stabilized by hydrogen bonds between hydroxyl groups and oxygens of adjacent molecules (Figure 1) [12]. Each monomer has three hydroxyl groups which grant some properties to cellulose's structure including hydrophilicity, chirality and biodegradability [13]. The ability of these hydroxyl groups to form hydrogen bonds controls the orientation of crystallinity and physical properties of cellulose.

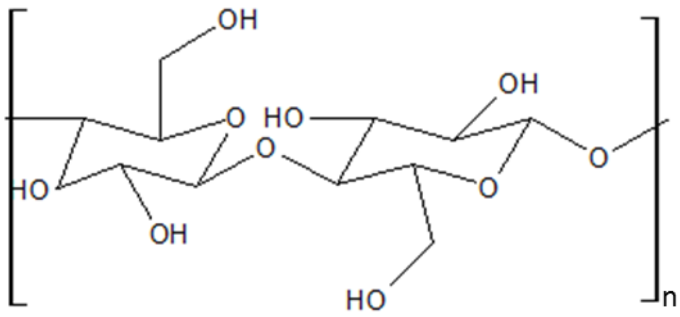


**Figure 1.** The chemical structure of cellulose

Cellulose has strong intra- and inter-molecular interactions between its polysaccharide chains resulting in its characteristic water insolubility. Thus, it has historically been used for numerous applications including composites, netting,

upholstery, coatings, packing, paper and in the pharmaceutical industry as a diluent/binder in tablets [14]. Nowadays the major utility of cellulose is for paper, membranes, tissues, scaffold material and textiles [15]. Cellulose is regarded as a relatively stiff and rigid polymer due its high viscosity in solution, a high susceptibility to crystallize, and capability to form fibrillar strands [3]. Native cellulose, which is produced by plants, is composed of two different polymorphs, Iα and Iβ. Iα cellulose is produced by bacteria and algae, while Iβ cellulose is the dominant polymorph in evolved plant species [16]. Various types of regenerated cellulose have been produced with high mechanical strength, excellent hydrophilic characteristics, good thermal resistance, and biodegradability [16]. Yet, to be more compatible with living agents, such as cell, enzyme, and functional polypeptide, cellulose based biomaterial needs further structural modifications. Significant efforts have been made in understanding the structural modifications of cellulose to improve its solubility and improve biopolymer stability by blending two or more polymers to obtain distinct properties [16-18].

**Chitin and Chitosan**

Chitin is another highly studied homopolysaccharide in the biomedical field which is the most widespread natural polymer next to cellulose. It is a hard, white in color, nitrogenous, and hydrophobic linear natural polymer consisting of (β1-4)-N-acetyl-D glucosamine repeat units (Figure 2) [3]. It naturally occurs as ordered crystalline microfibrils. These microfibrils make up the structural components in the exoskeleton of arthropods and in the cell walls of fungi and yeast [19]. The main commercial sources of chitin are crab and shrimp shells but it can also be found in many living organisms in the lower plant and animal kingdoms [19]. Annually, more than 100 billion tons of chitin

waste is produced by the crabbing and shrimp canning industry. The utilization of this waste was proposed for environmental protection as well as for a waste treatment alternative to the disposal process [20-22].

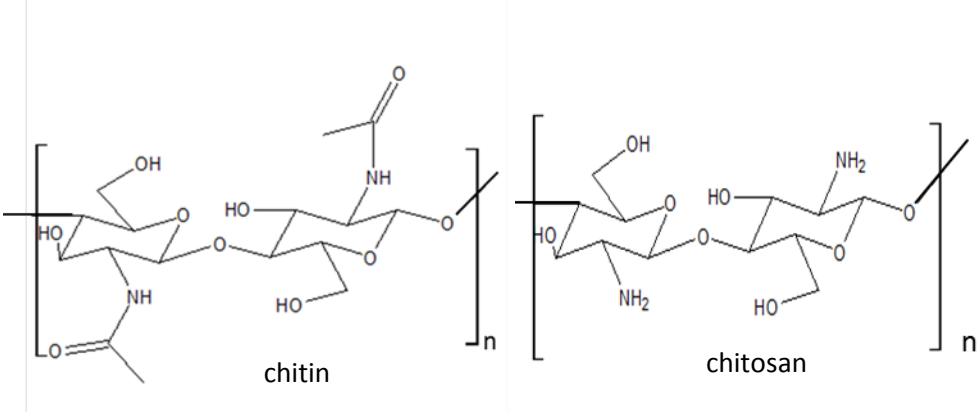


**Figure 2**. The chemical structure of chitin and chitosan

Chitin microfibrils are present in the structure varying in different orientations such as α-chitin, β-chitin and γ-chitin. In α-chitin the chains are anti-parallel while in β-chitin the chains are parallel. In the γ-chitin the chains are a mixture of both parallel and anti-parallel [23]. The β-form, which is less abundant than the α-form, is easier to dissolve and more reactive compared to the α-form. This is because there are no inter-sheet hydrogen bonds in the β-crystal [19]. These various type of formations result in different properties and can be distinguished by infrared and by solid-state NMR spectroscopy together with X-ray diffraction.

In general, most forms of chitin are highly hydrophobic and insoluble in water and most organic solvents, therefore it is difficult to process on an industrial scale due to its high crystallinity and strong intra-sheet hydrogen bonds [24]. Chitosan is a partially deacetylated (under alkaline conditions) derivative of chitin and is the most important

biosynthesized chitin derivative in terms of its applications [19]. Chitosan is also insoluble in neutral or basic conditions, while its protonated amine groups readily increase the solubility of chitosan in dilute acids (Figure 2) [3, 25].

Chitin and chitosan are also renewable polymers. Possessing this unique characteristic makes them valuable and useable for medical, pharmaceutical, cosmetic and wastewater treatment applications [19, 20, 26]. The insolubility of chitin makes it difficult to characterize and process, so several properties of chitin in the solid state have not been fully studied yet [19]. Generally, chitosan is much easier to process than chitin because of the free amine groups, but the stability of chitosan is lower due to the high hydrophilic groups. These compounds have reactive amine groups and reactive hydroxyl groups, which play critical roles in most chemical reactions by making effective hydrogen bonds. These linear biopolymers also have the ability to chelate metal ions, especially those of transition metals, by removing the cations from dilute solutions. This makes chitin and chitosan useful as a matrix for immobilization of enzymes [3, 19]. Moreover, these compounds are natural, safe, non-toxic, and biodegradable to normal body constituents. They can bind to mammalian and microbial cells aggressively, have a regenerative effect on connective tissue, and possess antifungal, antibacterial and antitumor properties [20]. Chitosan has similar structure to glycosaminoglycan (GAGs-an important component of extra cellular matrix), and for this reason it has been widely used in tissue engineering scaffolds [27].

In recent years, chitin and chitosan have gained attention for tissue engineering scaffolds and repairing damaged skin, but these applications are still under development [3, 26]. Chitin and chitosan have also been studied for clinical applications such as

artificial tissues and organs due to their biocompatibility. In particular, chitosan has been proposed to be generated as an artificial kidney membrane, because of its appropriate permeability and high tensile strength [3]. The primary recognized uses for chitosan are in the cosmetic and drug-delivery fields. For example, its mechanical stability, optical clarity, adequate optical correction, gas permeability, and immunological compatibility make chitosan the ideal material for contact lenses [3]. Chitosan is a great candidate for drug delivery because it is non-toxic, easily bio-absorbable in gel form, and has a low pH. All these characteristics may help them to prevent gastrodigestive issues for patients taking these medications [3]. It is also easier to process chitosan rather than chitin into forms such as capsules, sponges, and nanoparticles [26]. Chitosan films exhibit selective gas permeability and are resistant to fat diffusion; however, in terms of water transmission and water vapor, these characteristics are relatively poor due to chitosan's hydrophilic properties [26]. To overcome this problem, blending polymers in a multilayer system results in stable bioactive coatings of chitosan.

**Protein Silk**

Different types of polysaccharides have been incorporated in protein such as silk to mimic the naturally occurring environment of certain tissues [16, 28-32]. In the native tissues, the extracellular matrices (ECMs) are mainly composed of two types of extracellular polymers; fibrous proteins and proteoglycans. These both consist of a protein core covalently bonded to long chains of sulfated glycosaminoglycan GAG disaccharides [33]. Therefore, to fabricate protein such as silk one should be prepare to

acquire biomaterials that are able to perform mechanically and structurally like their biological counterparts [16, 33].

Silk is a well-known natural protein fiber produced by Lepidoptera larvae such as silkworms and spiders such as Bombyx mori [34]. It consists of two main proteins, hydrophilic sericin and hydrophobic silk fibroin. Fibroin is found in the core of the structure while sericin is found surrounding fibroin [33]. The core protein is made up of three structural chains: heavy chain, light chain and a glycoprotein. The light chain and heavy chain are linked by a disulfide bond. The light chain functions for the secretion of protein from the silk glands, while the heavy chain, also referred to as fibroin protein, functions for production of fiber protein and determines the properties of silk fiber [3]. Silk fibroin is a protein structure composes of 18 amino-acid sequence of predominantly Glycine, Alanine, and Serine. The combination of amino-acids varies from species to species which results in differences in the silks' chemical, structural, and mechanical properties [27, 33, 35]. For example, a sample of silk fibroin that possesses a high component of the poly-Alanine sequences have a more highly ordered crystalline structure which makes it less soluble in acid conditions, while a sample with poly-Gly-Ala sequences contains mostly beta-sheet regions (Figure 3) [35]. The silk fibroin has been a suitable biomaterial candidate for biomedical applications particularly for fabricating scaffolds for tissue regeneration. This is due to its compatible mechanical properties, ability to hold water vapor, oxygen permeability, blood compatibility, and biodegradability [27, 34]. However, pure silk fiber is brittle, so combining it with other materials is often needed such as in tissue engineering applications [29].

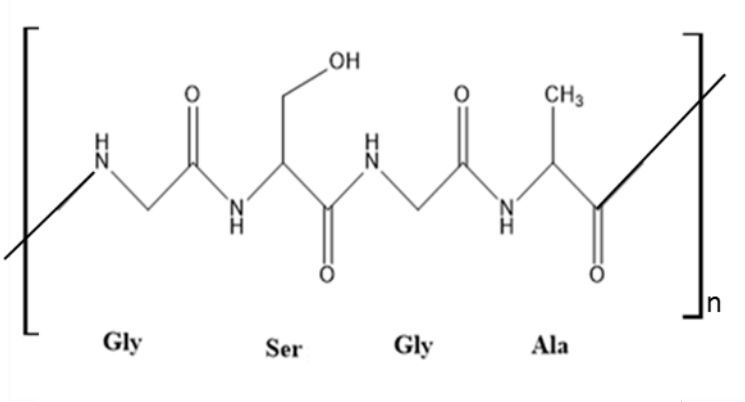


**Figure 3.** The chemical structure of silk fibroin

**Blend Polymers**

Blended systems based on silk fibroin and polysaccharides have been widely studied as an effective way to obtain desirable properties of each component [7, 16, 27, 32-34, 36]. The combination of silk with different polysaccharides has produced unique compounds that have proven to be valuable in biomedical engineering. Structural characterization methods aid to understand the interactions and behaviors of the regenerated biomaterials which leads to better control of the mixture process.

To utilize the biopolymers, it is necessary for the polymers to be dissolved in a solvent that is a suitable for its applications. As previously mentioned, cellulose, chitin and chitosan are insoluble in water and many organic solvents [24, 37]. It has been discovered that chitin and chitosan are soluble in hexafluoroisopropanol and hexafluoroacetone, however these solvents are not suitable for the biomedical field because of their toxicity [38].

**Ionic Liquids**

Ionic liquids (ILs) are an excellent alternative solvent which is used to dissolve natural polymers, therefore improving their ability to be processed [24, 34, 39, 40]. Scientists and engineers have tried to design materials with less hazardous and more environmentally friendly sources of energy production to decrease their environmental footprint [41]. The ILs are characterized as green solvents since they are non-volatile, non-flammable and recyclable [41]. In addition to being green solvents, ILs have gained popularity due to their chemical properties such as thermal stability, high ionic conductivity, negligible vapor pressure, and their easy recovery [34].

Theses solvents are salts, made up of a cationic and anionic component. The cationic species is responsible for certain chemical characteristics including the melting temperature and organic solubility, while the anionic species is responsible for the ILs air and water stability [42]. This leads to the facilitation of customizing ILs. The cationic part of ILs is characterized as a low bulky symmetric organic structure with a low melting point. Additionally, ILs are classified by their cationic group which falls into one of the following: 1) alkylammonium-, 2) dialkylimidazolium-, 3) phosphonium- and 4) N-alkylpyridinium. Cationic groups such as 1-allyl-3-methylimidazolium (AMIM), 1-butyl-3-methylimidazolium (BMIM) and 1-ethyl-3-methylimidazolium (EMIM), and anionic groups such as chloride, bromide, acetate, or formate have been reported as the most effective solvents for cellulose and chitin [24]. These imidazolium cations solvents differ from each other by the substitution of a unique side chain at position C1. The popularity of using the imidazolium ring as cation in ILs is due to its ease of synthesis, its

low viscosity, its stability within oxidative/reductive conditions, its unique properties as a catalyst, and its chemoselectivity for a variety of organic reactions [41].

In this study, we developed an understanding into how the thermal and morphological properties change as a function of material content and type of ionic liquid. We used ILs 1-allyl-3-methylimidazolium chloride (AMIMCl), 1-ethyl-3-methylimidazolium chloride (EMIMCl) and 1-ethyl-3-methylimidazolium acetate (EMIMAc) as solvents to dissolve cellulose/silk, chitin/silk and chitosan/silk. AMIMCl and EMIMCl have the same anionic group, chloride, but have different cation groups which connect to the imidazolium ring; EMIMCl has ethyl group while AMIMCl has the unique double bond that could enhance its reactions between the biomaterials and the IL (Figure 4). EMIMAc and EMIMCl share the same ethyl substitution (cation) but differ in the type and size of the anion group. The variations on the cation and/or anion can adjust the physical property of the ILs [42]. For example, it has been found that as the size and the asymmetry of the cation and anion increases, the melting point decreases. In our investigation, the regenerated films were characterized using Attenuated Total Reflectance Fourier Transform Infrared spectroscopy (ATR-FTIR), Thermogravimetric analysis (TGA), Scanning Electron Microscope (SEM) and Differential Scanning Calorimetry (DSC).

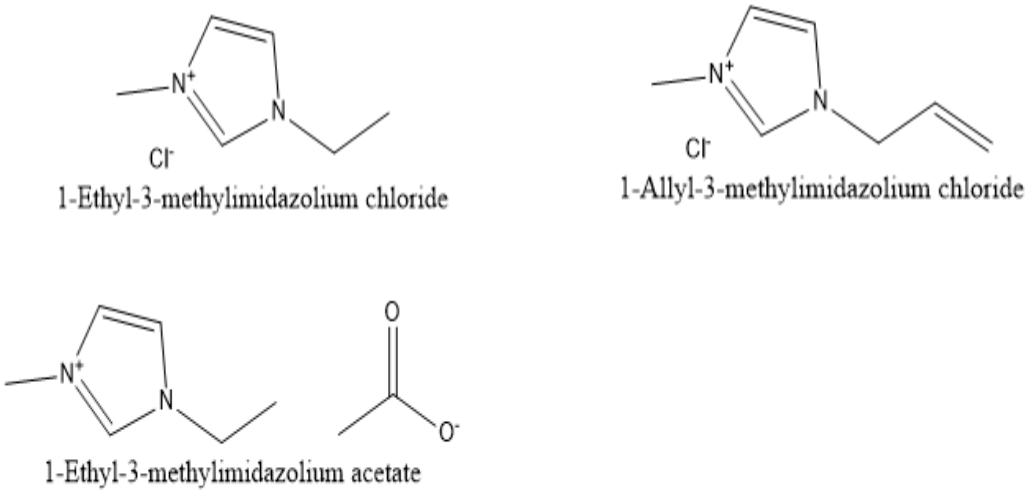


**Figure 4.** The chemical structure of Ionic Liquids used in this study

# Chapter 2: Comparing the Interactions and Thermal Effect of Polysaccharides/Protein-Based Films In 1-Allyl-3-methylimidazolium Chloride as a Function of Material Composition

## Introduction

Interest in researching and developing dynamic biomaterials for tissue engineering and environmental science has expanded in recent years due to increase in the demand of skin damage treatment and air and water pollution detection and remediation system, respectively. Biomaterials are categorized into two groups: natural and synthetic. Naturally derived biomaterials, such as polysaccharide-based (cellulose, chitin, chitosan) and protein-based (silk) biomaterials, have shown to be preferable over synthetic biomaterials for human applications [3]. Blending polysaccharides with proteins can mimic the natural environment of certain tissues [34, 43].

For the past 10 years, biopolymers, such as cellulose, chitin and its derivative chitosan, have shown potential for applications in drug and gene delivery, biomedical treatment, cosmetic, and heterogeneous catalytic [3, 26]. Cellulose, which consists of repeating glucose units connected by (β1-4) glycosidic bonds, is the most abundant renewable material and has been used in various applications such as biomedical research, fuel production, and 3D printing [18]. Chitin is the second most abundant natural biopolymer, containing the monomer (β1-4)-N-acetyl-D-glucosamine [19]. Annually, crustaceans, mollusks, insects, fungus, and certain algae produce more than 100 billion tons of chitin, with the main commercial source being shrimp and crab shells [21]. Chitin is a hard, white, inelastic nitrogenous hydrophobic linear polymer. It is

difficult to dissolve in conventional solvents and to produce on an industrial scale because of its high crystallinity and strong inter-and intra-molecular hydrogen bonding sheets [3, 24]. Chitosan is a partially deacetylated (under alkaline condition) derivative of chitin and is the most important practical chitin derivative [3, 19]. Chitosan has been utilized in hair and skin care products as well as environmental protection such as remediation of organic and inorganic contaminants including toxic metal and drugs in polluted waters [44, 45]. Structurally, chitosan is very similar to chitin and cellulose, they differ only at position carbon 2. For example, chitin has acetamido functional group, chitosan has the amine functional group and cellulose has the hydroxyl functional group. Even though the three polysaccharides share the (β1-4) anhydroglucosidic bond, cellulose demonstrates very different characteristics than either chitin or chitosan. Yet, all of these polysaccharides have two allomorph forms α and β, which can lead to different properties [34, 46]. These biopolymers can be distinguished by infrared and solid-state NMR spectroscopy together with X-ray diffraction [19]. Chitin and chitosan have advantageous chemical properties such as strong reactivity of amine and hydroxyl group, chelation with many transition metal ions, and contains medically desirable properties such as nontoxicity, biocompatibility, biodegradability, and antitumor, antibacterial, and antifungal activity [20, 26].

Silk proteins such as the Mori silk are a unique well-known biopolymer produced widely by silkworms and spiders [28, 34]. It primarily consists of a hydrophobic fibroin wrapped up by hydrophilic sericine [27]. Silk fibroin is a fiber composed of 18 amino acids such as glycine, alanine, serine [27]. Silk fibroin has many advantageous features, like strong mechanical properties, oxygen, and water vapor permeability,

biocompatibility, and biodegradability. These various features of silk fibroin can be manipulated and applied in tissue regeneration and biomedical applications [27]. Moreover, silk bio-polymerase is already utilized to create matrices for wound healing due to its crystalline structure that reflects UV radiation and acts as productive buffer between the skin and environment [3]. However, pure silk fiber is brittle, so combining the biopolymer with other materials, such as a polysaccharide, is often employed in tissue engineering applications [29]. To utilize cellulose, chitin, chitosan and silk in a diverse range of applications, it is essential to compose stable homogenous films in order to develop effective modification of these biopolymers. However, the strong intra-and intermolecular forces of these biopolymers decrease their solubility in many organic solvents [40]. Some studies have attempted to use organic solvents such as hexafluoroisopropanol (HFIP) or hexafIuoroacetone to dissolve chitin with protein silk to obtain homogenous films [47]. Yet, these solvents have limited application due to high toxicity and difficult removal [38].

Ionic liquids (ILs) have been shown to be excellent alternative solvents for these natural polymers, improving their processability [24, 34, 39]. Ionic liquids are defined as group of organic salt compounds that are liquids at room temperature, have low melting points, and dissolve natural polymers [24]. These ILs have an imidazolium-based cation such as [AMIM] (1-allyl-3-methylimidazolium), [EMIM] (1-ethyl-3-methylimidazolium), or (BMIM) (1-butyl-3-methylimidazolium) and an anion such as chloride, acetate, or bromide. ILs are attractive solvents due to their amenable properties including high thermal mechanical electrochemical stability, very low vapor pressure,

easy separation, low toxicity, and non-volatile [42]. In this study, we chose AMIMCl as a solvent due to its recent success at blending cellulose with other biomaterial [18, 48].

Considering the desirable properties of chitin, chitosan, cellulose and silk, a film composed of two polymers instead of one might mimic the naturally occurring environment of certain tissues [27, 34]. The characterization of blended structures based on silk fibroin/chitin, silk fibroin/chitosan, and silk fibroin/cellulose with various ratios using ILs have not yet fully explored [34, 49]. For instance when silk is mixed with an individual polysaccharide, the silk's amino acid groups function as binding sites for the polysaccharide, which improves the toughness and stability of the materials with no substantial change in the chemical properties of the either polymers [49]. ILs can be easily removed from these products using ethanol or water, leaving behind effective materials that might be used in biomedical applications. As mimicking the natural scaffold of the exoskeleton of shrimp, once the ILs have been removed, the amino groups in the silk structure can rearrange and wrap around the polysaccharide monomer. This new configuration of silk-polysaccharide gives a combination of the two polymers' properties. Changing the ratio of the silk/polysaccharide films can obtain structural modifications which affect the thermal stability and the topography of the films. Understanding the interactions between polysaccharides and protein and how the structures can be modified may contribute to innovative engineering designs. We aim to mimic the organic phase of the insect cuticle and the exoskeleton of crustacean by making polysaccharide nanofibers embedded in a silk-like protein matrix. In this study, the formation of the blended polysaccharides-silk films (cellulose/silk, chitin/silk, chitosan/silk) that dissolved in AMIMCl were investigated using various techniques

including FTIR, TGA, SEM, and DSC. Moreover, based on the different substituents in each polysaccharide's backbone at carbon 2, we have observed different film formation with silk despite the similarity of the other 5 carbon substituents. The goal of this study is to characterize, understand and compare the behavior of each blending polysaccharides individually (cellulose, chitin and chitosan) with silk using AMIMCl by characterizing the modification of structure via thermal properties and topography.

## Material and Methods

### Material

Silk: The protein was provided by Dr. Xiao Hu from Rowan University, Cellulose: Avicel microcrystalline cellulose (Techware: Z26578-0) was acquired from Analtech (Newark, DE, USA), Chitin: Chitin from shrimp shells was purchased from Sigma (C7170), Chitosan: Chitosan was purchased from Sigma (448877), Ionic liquid: 1-allyl-3-methylimidazolium chloride (AMIMCl) was purchased from Alfa Aesar.

### Experiment

AMIMCl was placed in a test tube (approximately 95 w/w). Then the tube was placed on a hotplate. α-Chitin/chitosan/cellulose and silk were added individually (about 5 w/w), and the experiment was conducted at a temperature between 100-105℃ for 48 hours using magnetic stirring. The blended films were transferred between two glass slides. Water was added to the films to regenerate the polysaccharide /silk films and the samples were kept in water for another 48 hours to remove as much IL as possible. The films were dried for 24 hours in a vacuum oven at 50℃.

## Characterization Methods

### Attenuated Total Reflectance Fourier Transform Infrared spectroscopy (ATR-FTIR )

Fourier transform infrared Spectra (FTIR) analysis was performed using Bruker ALPHA-Platinum FTIR Spectrometer, with Platinum-Diamond sample module using Bruker OPUS Mentor Plus software version 7.2, Build: 7.2.139.1294. The spectra were collected in the wavenumber between 400-4000 $cm^{-1}$, resolution 4 $cm^{-1}$, 32 sample scans and 128 background scans. Six different locations were analyzed for each sample and averaged together. The percentage of the crystallinity of beta sheet of silk was obtained from each sample by selecting the Fourier Self Deconvolution, and the frequency range was set between 1700-1500 $cm^{-1}$ to enable the spectrum to be interactive in the selected wavenumber [50]. Then parameters were set as the following: Noise reduction 0.30 and Bandwidth 25 using a Lorentzian, Local Least Square and Gauss shape methods. To obtain the crystallinity of beta sheet, the sum numbers of beta sheet were divided by the sum numbers of the integral.

### Thermogravimetric analysis (TGA)

Thermal data was obtained using Thermogravimetric Analysis (TGA) which was carried out on TA Instruments Discovery system, performed on all samples in a nitrogen atmosphere. The heating process was run at 10℃/min ramp to 650℃ for average sample of 6mg. The software determines derivative plot by using the peak height analysis.

Differential Scanning Calorimetry (DSC)

Samples (approximately 5mg) were enclosed in TZero aluminum pans and run in a TA Instruments Discovery with a Refrigerated cooling system (RCS) and with nitrogen gas flow (25 mL $min^{-1}$). The standard Aluminum reference was used to calibrate the heat capacity. Samples heated from 5℃/min up to 120℃ to allow the water to evaporate. They were then cooled down to -30℃, and heated up again to 170℃.

Scanning Electron Microscope (SEM)

The SEM images were taken on the LEO1450EP SEM at Rutgers University Camden campus. A small piece was mounted on carbon tape on Denton Desk II Au-Pd sputter coater. The samples were sputter coated and run in a light-vacuum of 10V for 60 seconds. The magnification used in this paper is a scale bar of 2000x (10.00μm).

## Results and Discussion

### Structural Analysis

The observable morphology of the regenerated films differed according to the polysaccharide/protein composition: cellulose/silk films were characterized as firm and solid while chitin/silk and chitosan/silk films were soft and powdery. Table 1 displays the concentration of silk used in this paper. The various compositions were chosen to test the crystallinity of beta sheet and how these ratios could affect the interactions between chains and the ability of the amino acids to wrap around the individual polysaccharides. Our hypothesis is that as silk content increases the ability of the silk's amino acids to

wrap around the polysaccharide monomer will increase. AMIMCl, cellulose, chitin, chitosan and silk each have a unique IR spectrum as shown in Figure 5. For example, the major peaks of cellulose are common to all polysaccharides, the broad regions of OH (3500-3000 $cm^{-1}$) and C-O (around 1100 $cm^{-1}$). Alternatively, chitin and chitosan share amide peaks at around 3200 and 1600 $cm^{-1}$ [51], this is also observed in the pure silk structure. The major peaks at 3050, 2965, 1570, and 1165 $cm^{-1}$ are characteristic of AMIMCl [52].

| **Polysaccharide** | **Silk** |
|---|---|
| Cellulose 80% | 20% |
| 20% | 80% |
| Chitin 80% | 20% |
| 20% | 80% |
| Chitosan 80% | 20% |
| 20% | 80% |

**Table 1.** Experimental conditions of the relative concentration of polysaccharides and silk

With the 20% silk films, the FTIR spectra indicates conformational modifications for the structures at the molecular level, possibly due to structural rearrangement of the chains when compared with the pure component as shown in Figure 5. It is important to

note that the ease of dissolution of polysaccharides in AMIMCl varies depending on the functional group and crystallinity of the given polysaccharide. Cellulose tends to dissolve more easily in AMIMCl [18, 53] when compared with chitin and chitosan. Youngs et al. suggest there is a small favorable van der Waals energy contribution between the sugar and cations (imidazolium ring) [53]. Thus, the spectra elucidate sharper peaks related to the cation part of the ionic liquid (N-C aromatic ring) at the wavenumber of 1165 $cm^{-1}$ stacking between chains in all the structures of all polysaccharide blended bio-composite films. As shown from IR spectra in Figure 5, the blended films have more intense absorbance compared with the pure component, and there are some peaks (amide I and II regions, 1576-1646$cm^{-1}$) appear in cellulose/silk 20% (CES20) film, which did not appear in the pure cellulose spectra. This can be explained by the hydrogen bonding that occurs between hydroxyl groups in cellulose and the cation groups in the AMIMCl and between hydroxyl groups in cellulose and the amine groups in silk. Moreover, the spectra illustrate an increase in the absorbance of the amide I and II regions (between 1576-1646 $cm^{-1}$) when 20% silk was added to all three polymers, as seen in Figure 5. Unlike the spectra of CES20 film and chitosan/silk 20 (CTS20) film, the amide III peak (1260 $cm^{-1}$) is intense in chitin/silk 20 (CHS20) film, which may contribute to the extra strong hydrogen bonding chitin forms with fiber silk [28].

At first there seem that no significant change in IR spectra between 80% silk films and 20% silk films within the same polysaccharide, as seen in Figure 6. The major obvious change is in cellulose/silk 80% (CES80) film, the amide I peak has higher intensity than amide II peak which is contrary to the CES20 film that has higher intensity of amide II peak than amide I peak. Even though the spectra appears to be identical

between the 20% and 80% silk films for both chitin and chitosan, there is a difference in crystallinity. When the crystallinity of the beta sheet was calculated using Local Least Square and Gauss shape methods [50], the crystallinity of the beta sheet increased when the amount of silk increased from 20% to 80% silk for each polysaccharide (Table 2). Therefore, it can be determined that the interactions between silk and polysaccharides increase the crystallinity of the beta sheet, for as the silk ratio increase from 20% to 80% the crystallinity values increase in proportion to the percentage of silk in the film.

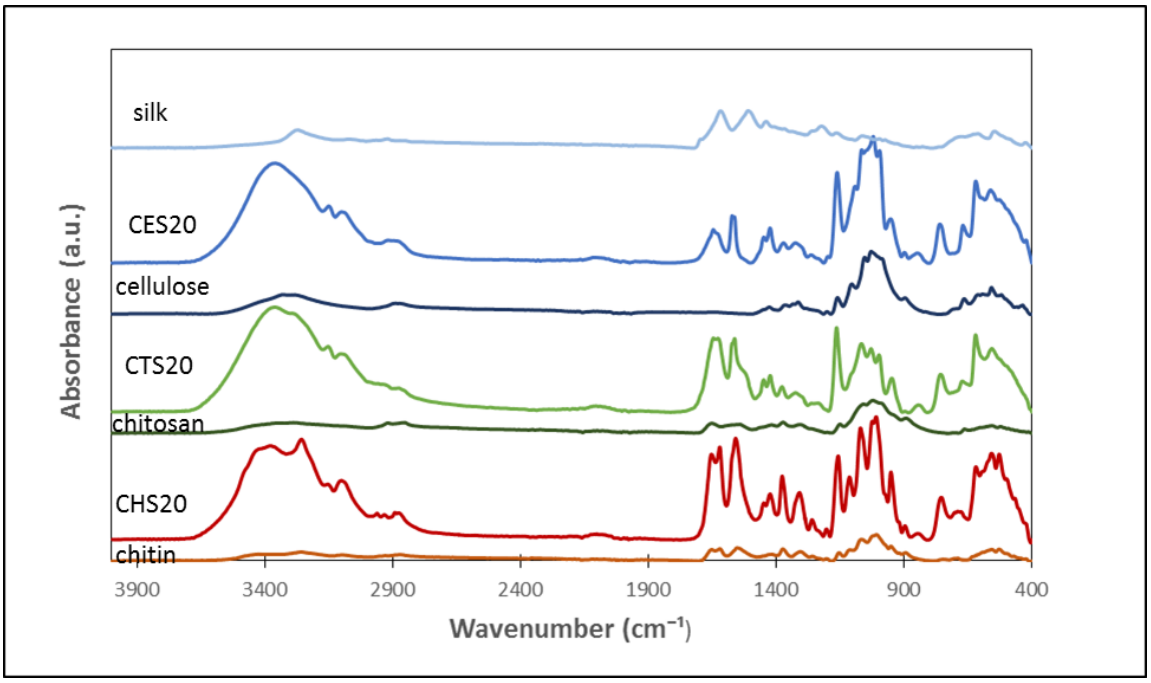


**Figure 5.** The comparison of IR spectra for the pure polysaccharide chitin, chitosan cellulose and protein silk, with spectra for the blended films chitin/silk 20 (CHS20), chitosan/silk 20 (CTS20), cellulose/silk 20 (CES20)

Beta sheet of silk interacts differently with chains of cellulose, chitin and chitosan. In cellulose blended films, the crystallinity of beta sheet increases from 28.4% in CES20 to 37.6% in CES80. While in chitin blended films, the crystallinity increases

from 22.4% (CHS20) to 42.2% chitin/silk 80 (CHS80), and in chitosan, the number grows from 18.1% (CTS20) to 31.3% chitosan/silk 80 (CTS80). As a result, the ratio of the beta sheet elevates by 9.2 % as the amount of silk increases (20% to 80%) in cellulose-silk films. Alternatively, in chitin-silk films, the ratio jumps by 19.8%, and chitosan-silk films gets the moderate ratio between cellulose-silk and chitin-silk films 13.2%. This could be due to the higher likelihood of interaction between the chitin chains and silk fiber relative to either cellulose or chitosan because of chitin's acetamido function that makes it available to hydrogen bond with silk chains. Overall, absorbance increases in the amide (I, II) area as the amount of silk ratio increases from 20% to 80% silk in cellulose, chitin and chitosan as shown in Figure 6. The increase in the absorbance of the amide region proved that there are some interactions between beta sheet in silk and polysaccharides caused by hydrogen bonding. Consequently, the crystallinity of beta sheet will rise for cellulose, chitin and chitosan. The highest jump in crystallinity of beta sheet is shown by chitin/silk films (CHS20 to CHS80).

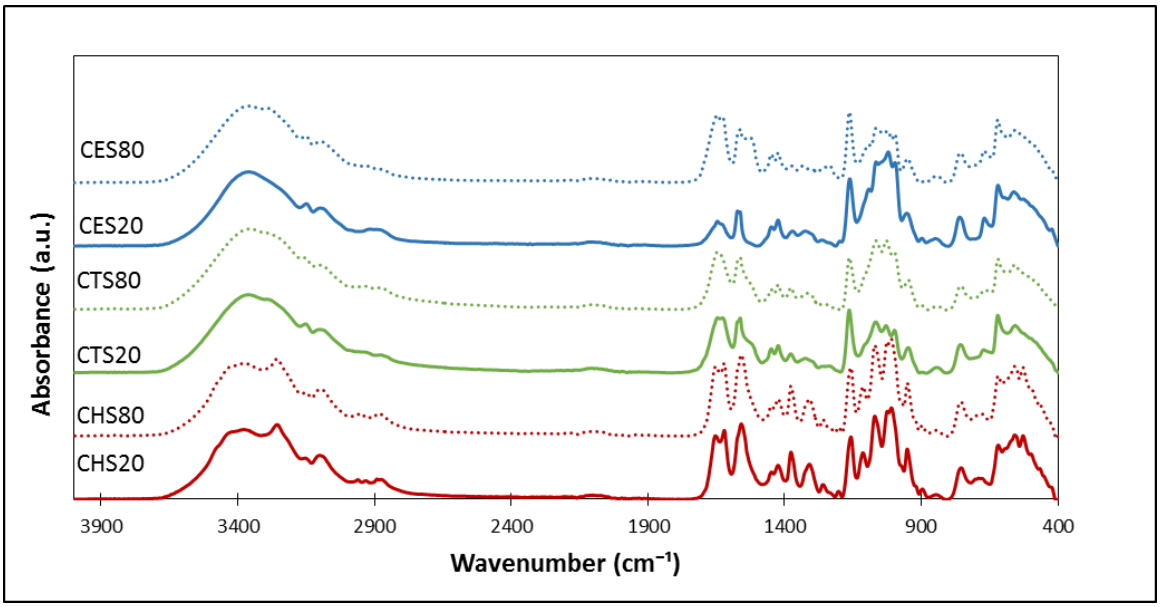


**Figure 6.** The IR spectra of 20% silk films cellulose/silk 20 (CES20), chitosan/silk 20 (CTS20), chitin/silk 20 (CHS20), and the spectra of 80% silk films cellulose/silk 80 (CES80), chitosan/silk 80 (CTS80), chitin/silk 80 (CHS80)

| Polysaccharide | Crystallinity of beta sheet in 20% silk film | Crystallinity of beta sheet in 80% silk film | The difference in crystallinity |
|---|---|---|---|
| Cellulose | 28.4% | 37.6% | 9.2% |
| Chitin | 22.4% | 42.2% | 19.8% |
| Chitosan | 18.1% | 31.3% | 13.2% |

**Table 2.**The percentage of crystallinity of beta sheet blended films at 20 and 80% silk and the crystallinity differences.

**Morphology Analysis (SEM)**

As can be seen in Figure 7, the SEM images demonstrate the topological changes in film morphology as the proportion of silk changes in each polysaccharide. In Figure 7, the films with higher amounts of silk (80% silk) have smoother surfaces than films with less silk (20% silk) [34]. As previously discussed, the polysaccharides share very similar backbone structures. For instance, the difference between chitosan and cellulose is that chitosan has an amine group at position 2 and cellulose has a hydroxyl group. This impacts the morphology of the films, with cellulose film presenting a more fibrous structure surface (Figure 7 CES20) while chitosan films demonstrate a more porosity construction surface (Figure 7 CTS20). In accordance with the FTIR results that demonstrate chitosan-silk films containing moderate crystalline beta sheets (1576-1646 $cm^{-1}$), the pores morphology of chitosan-silk films indicate that polymeric chains are disrupted, making a space between chains. The surface of chitin-silk film (Figure 7 CHS20) reveals some divided parts (cuts), which may be an indication of chitin's backbone chains expanding during the mixing process. These insights gained from SEM images match the IR spectra patterns analysis.

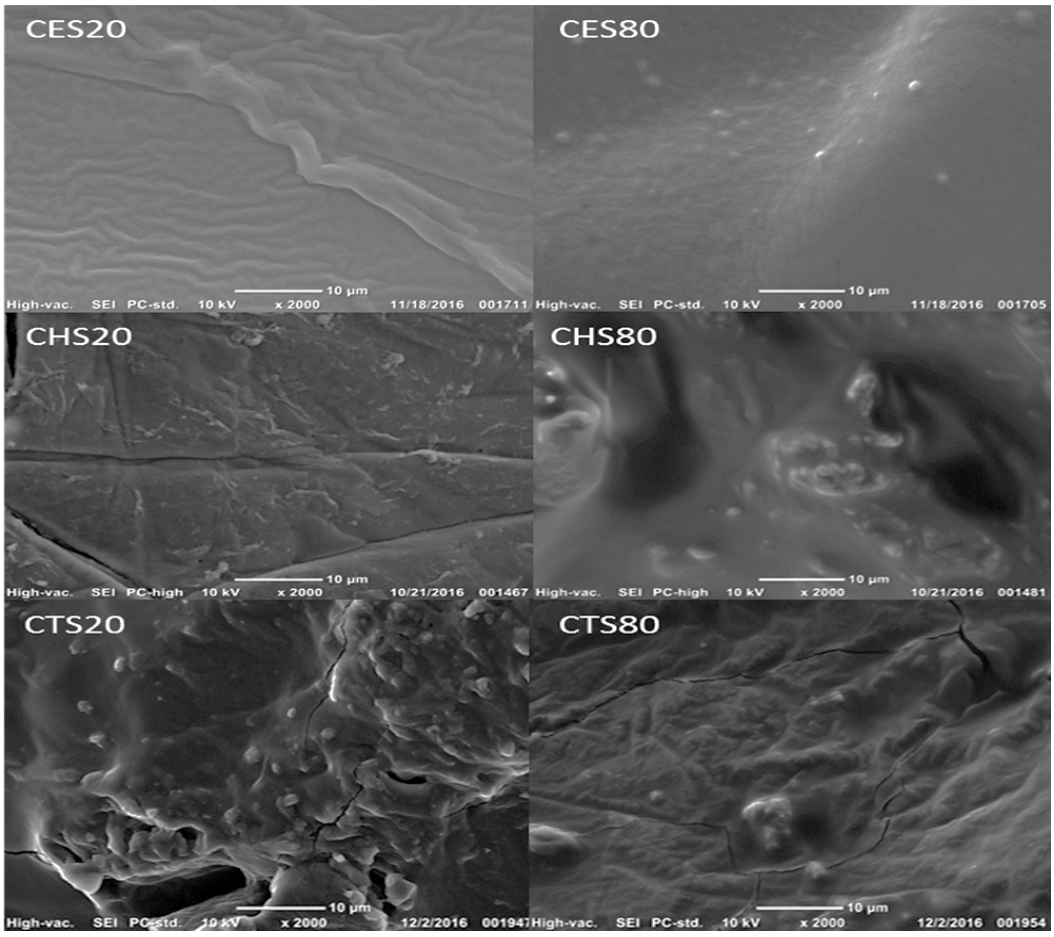


**Figure 7.** SEM images for polysaccharides/silk films at 20% and 80% silk (CES20), (CES80), (CHS20), (CHS80), (CTS20), and (CTS80)

**Thermal Analysis (TGA)**

TGA experiments enabled further characterization of structural modifications based on thermal stability and structural strength, as measured by decomposition temperatures. The TGA curves depict thermal degradation temperatures for pure microcrystalline cellulose, chitin, chitosan, silk and for the blended films (Figure 8). Obviously, the thermal degradation of the pure polysaccharides component shows that chitosan has less stability when compared with cellulose and chitin. The initial weight

loss below 100 ℃ is because of water evaporation [49, 54]. The thermogravimetric analysis of pure chitin reveals its two-stage decomposition processing, with a first maximum at 287 ℃ and a second maximum at 396 ℃ [55]. Alternatively, pure cellulose and chitosan display one phase degradation, with maxima at 363 ℃ and 288 ℃ for cellulose and chitosan, respectively (Table 3). From Table 3, it should be noted that the 20% silk films have two maximum decomposition temperatures for all polysaccharide films, while in 80% silk films the chitosan film (CTS20) is the only film that has two decomposition temperatures. Generally, the main observation of the curves in Figure 8 is that the decomposition of the blended films occurs at the lower temperature than the pure material component, which is due to the chain disruption causing stability changes. Furthermore, increases in the silk content (20% to 80% silk) in the blended films slightly increases the temperature of thermal degradation, indicating that silk content provides a thermal stability in the blended films due to an increase in percent crystallinity as shown in the FTIR section [32]. Interestingly, the minor degrading step occurs over 350 ℃ in the CHS20 film and below 300 ℃ in the pure chitin. This could be interpreted by the decomposition of acetamido group [55], and the amorphous chains may happen at the first (minor) decomposition step in the pure chitin. The minor decomposition in CHS20 film could be related to the very hard crystalline region that did not disrupt during the mixing process. However, the CHS80 film decomposed in one step.

The maximum temperature decomposition of blended films varied according to the amount of silk. As seen in Table 3, the maximum decomposition increases slightly when the amount of silk increases (20% to 80%) in all blended polysaccharides. The higher change in temperature (based on the first decomposition) is in chitin films (CHS20

to CHS80) by 10℃, giving supportive evidence for the IR results. Whereas the lowest temperature change is in cellulose films (CES20 to CES80) by 3℃, and chitosan films (CTS20 to CTS80) has the intermediate temperature change among chitin and cellulose films with 7℃. Moreover, in both 20% and 80% silk films, the appearance of the shoulder in the derivative peak for chitosan films could be attributed to the free amine groups in chitosan and free amide groups in silk weakly interacting during degradation.

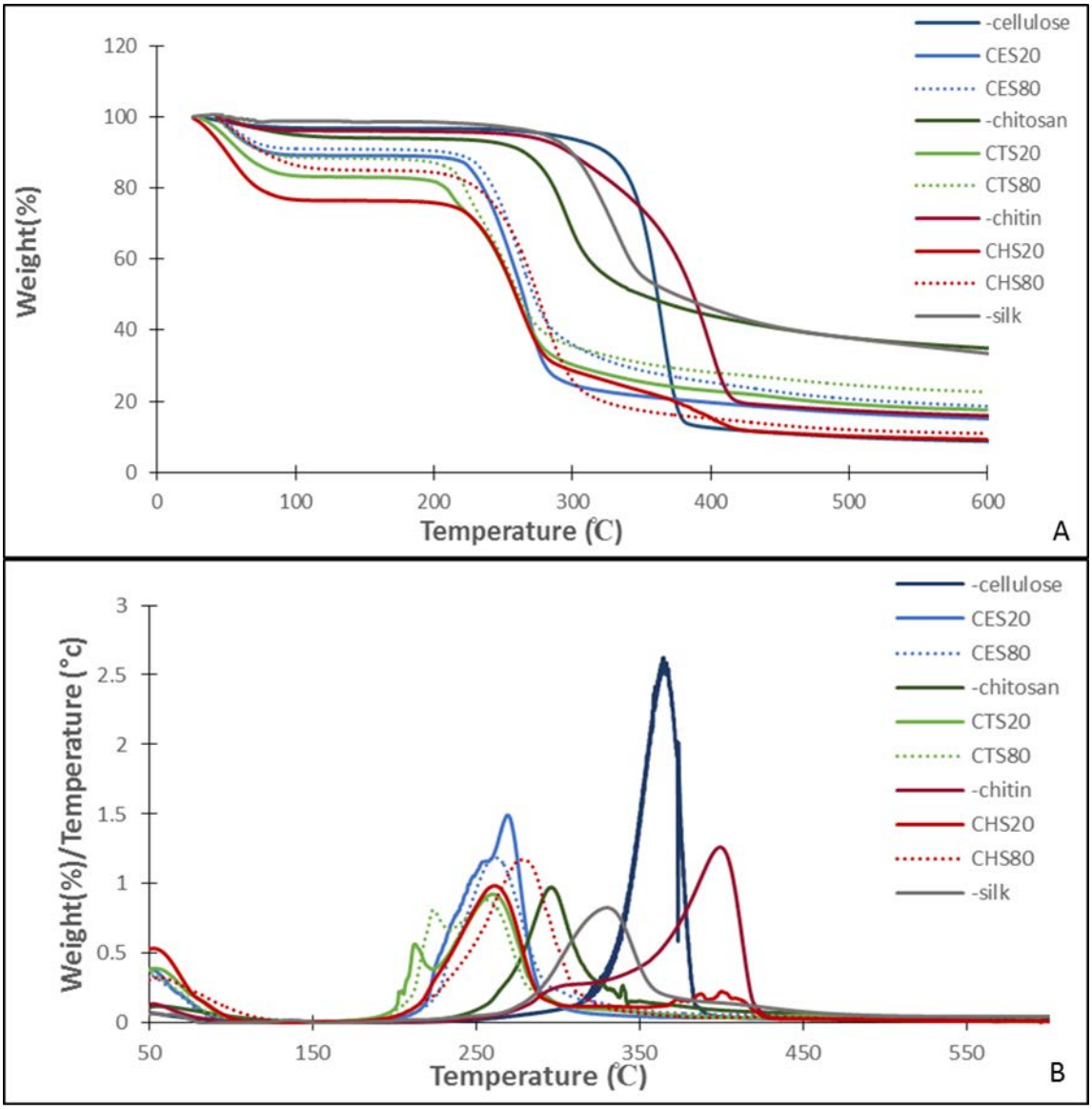


**Figure 8.** The thermal degradation of the pure polysaccharide, silk and blended films A) percent weight decomposition, B) derivative percent weight decomposition.

| Sample | Maximum decomposition (1) ℃ | Maximum decomposition (2) ℃ |
|---|---|---|
| 1-pure | | |
| Cellulose | 363 | - |
| Chitin | 287 | 396 |
| Chitosan | 288 | - |
| silk | 322 | - |
| 2-20%silk film | | |
| CES20 | 255 | 268 |
| CHS20 | 266 | 386 |
| CTS20 | 217 | 254 |
| 3-80%silk film | | |
| CES80 | 258 | - |
| CHS80 | 276 | - |
| CTS80 | 224 | 259 |

**Table 3.** The maximum decomposition of the pure polysaccharides, silk and the blended films

**Thermal Analysis (DSC)**

Figure 9 shows the DSC thermograms for the blended films. It can be noted that the water evaporation peak ($T_w$) appears more obvious and broad in chitosan films than cellulose and chitin films. For chitosan films, the range of $T_w$ is around 70-170℃ and for cellulose and chitin films is around 80-130℃. We need to remember that the presented data represents the second cycle in the DSC protocol; hence, $T_w$ can be associated with the glass transition temperature ($T_g$). This typical result was observed in the TGA data where about 7 to 10% could be accounted to water loss. Thus, we could assume that the higher and broad $T_w$ peak in chitosan films correlated to the great pores in the surface of the SEM image. Alternatively, cellulose and chitin films exhibit less magnitude in this area. The $T_g$, for pure silk is around 180℃ and for pure chitin is around 130℃ [56, 57]. The strength of water holding capacity increases with increase in N-deacetylation (going from chitin to chitosan) due to the free hydrophilicity groups of amine in chitosan [57]. In cellulose and chitin, the initial water molecules are associated with hydroxyl groups, as the free amine present in the system (chitosan), the newly created hydrophilic center is present and the number of water molecules bound to the chains increase.

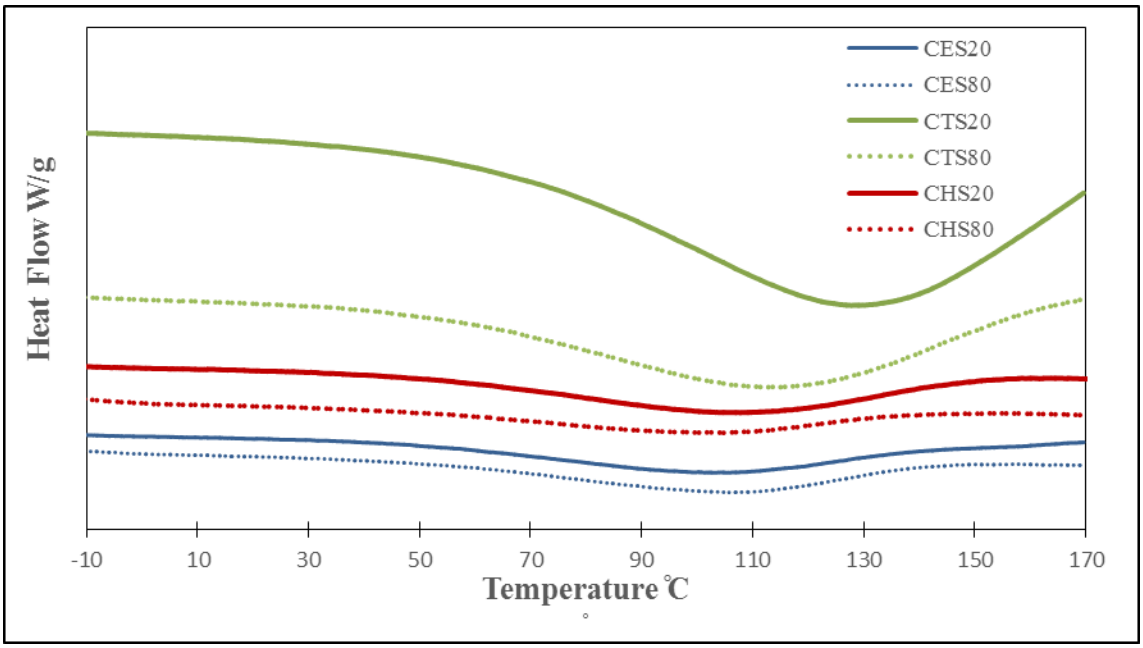


**Figure 9.** DSC curves of blended films at 20% and 80% silk concentration

## Conclusion

Here, we have investigated and compared the effect of high and low concentrations of blended silk films using three different polysaccharides and the ionic liquid 1-allyl-3-methylimidazolium chloride (AMIMCl). The importance of these biopolymers (cellulose, chitin, chitosan, silk) resides in their biological properties (biodegradability, biocompatibility and non-toxicity). The blended polymer technique offers distinct properties arising from the desirable characteristic of both protein (silk) and polysaccharides (cellulose, chitin and chitosan), improving the stability and strength of the material. We can conclude from this study that increasing the silk content in the polysaccharides can increase the molecular interactions between the biopolymers, causing an increase in the stability of the blended film. Even though there is no significant change in IR spectra between 80% and 20% silk in chitin and chitosan films,

the calculation of the crystallinity of beta sheet shows significant changes as amount of silk increases. In addition, chitin films show the highest beta sheet crystallinity going from 20% to 80% silk. The TGA results also illustrate that the thermal stability is higher for the chitin films as compared to chitosan and cellulose films. The low concentration chitosan film (20% silk) has more pores surface in SEM image, which may correlate to its lowest thermal stability and high water absorbance. By understanding the effect of structural and thermal stability based on polysaccharide as a function of silk content, the behavior of different blended films facilitates the development of customized blended structure for each tissue engineering and environmental pollution detection and remediation applications.

**Abbreviation: Cellulose/silk 20(CES20), cellulose/silk 80 (CES80), chitin/silk 20 (CHS20), chitin/silk 80 (CHS80), chitosan/silk 20 (CTS20), chitosan/silk 80 (CTS80)**

# Chapter 3: Comparing the Structure and the Thermal Behavior of Chitin/Silk Composite Films as a Function of Ionic Liquid Type

## Introduction

Natural polymers have been studied and utilized for the past two decades. Typical examples, such as bone, tooth, wood, arthropod cuticle, and crustacean exoskeleton are natural structural materials that are the inspiration for sustainable structural composites [22]. These biopolymers are assembled to produce a complex hierarchical structure that has the advantageous chemical properties of strength and toughness [28, 43]. Many studies have tried to mimic their naturally occurring environment by blending polysaccharides and protein to obtain various materials that can be used in applications suitable for biotechnological, biological, biomedical and environmental applications [16, 27, 28, 32, 34]. Yet, the modification and relationship between physicochemical properties and morphology of blended biomaterial structures has not been fully explored. These natural polymers (e.g. polysaccharides or protein) accomplish diverse functions in the natural world. For example, polysaccharides function in the aggregation of the extracellular matrix, and proteins are multi-adhesive with different matrix molecules and function as a catalyst.

Among the natural polysaccharides, chitin is a homopolysaccharide, which contains only a single monomeric species. It is the most widespread biopolymer after cellulose, composed of 2-acetamido-2-deoxy-β-D-glucopyranose repeating units. Chitin has limited applications due to insolubility and high crystallinity of the polymer [24].

Many studies have tried to dissolve it, or to modify its monomers to improve its solubility [24, 40, 58]. To improve chitin solubility, it has been deacetylated to chitosan, which is a linear deacetylated derivative of chitin, and widely used in tissue engineering and wound-healing applications [29, 34]. It has structural similarity with glycosaminoglycans (GAGs—an important component of the extracellular matrix (ECM)), and has antimicrobial and hemostatic properties [27, 34]. Chitin and its derivative chitosan have shown tremendous promise as tissue-bracing substances [59]. The stability of chitosan is inferior than chitin due to its high hydrophilic groups [19]. Chitin has been blended with proteins to mimic the scaffold of the insect cuticle and the exoskeleton of crustaceans to replace damaged tissues due to its stable, tough and strong structure [28]. In comparison to the hydroxyl and ether groups that cellulose possessed, chitin has acetamido groups that can play a role in the blending processes originated by extra hydrogen bonds as seen in the previous chapter.

Silk is a widely-used protein often blended with polysaccharides to obtain materials that are strong enough to support cellular growth [16, 27, 30, 32-34]. It is made of fibrous proteins produced by silkworms [60]. Silk fibroin, which is the core of silk fiber, is composed of highly sequenced hydrophobic amino acids groups. Silk's physical and chemical properties are affected by the molecular conformation of silk fibroin, so to control these properties, the molecular conformation needs to be considered [32]. Silk I and silk II are the two types of molecular conformation of the secondary structure of silk fibroin. Silk I is a non-crystal, random, coil α-helix and is water-soluble while silk II is a highly organized stable β-sheet conformation, insoluble in water. Despite these differing properties, both conformations are present in silk fibroin product [32]. Silk fibroin is

considered to be an appropriate substance for use in the biomedical field due to properties such as good water vapor and oxygen permeability, blood compatibility, and improvement of collagen deposition and fibroblasts proliferation [34]. Recently, different types of regenerated silk fibroin-based bio-material have been used in many applications including membranes, gels, and scaffolds [61]. However, in solutions, intermolecular hydrogen bonds are not enough to stabilize the silk fibroin structure, and it is characterized as brittle. To improve the properties of silk, a blended system with polysaccharides has been suggested [30, 31]. One study fabricated a chitin-silk bio-composite to yield homogeneous films using hexafluoroisopropanol (HFIP) or hexafIuoroacetone as a solvent [28], but these solvents are not suitable for the biomedical field because of their toxicity [38].

It is necessary to choose a suitable solvent to dissolve and blend these biomaterials. Ionic liquids (ILs) are group of organic solvents that have been shown to work effectively for dissolution of natural polymers [18, 24, 34, 40, 42, 53]. With developing awareness of environmental protection, researchers are directed to replace traditional volatile organics with more environmentally friendly or “green” solvents, so ILs have been selected as the replacement [42]. In addition, ILs have been chosen due to their desirable properties such as high thermal, mechanical, and electrochemical stability, very low vapor pressure, easy separation, low toxicity, and non-volatility [42]. The imidazolium-based ionic liquids have been selected as a more effective solvent of the natural polymer of chitin [30, 34]. IL’s physical and chemical properties are controlled by their positive (cation) and negative (anion) charges [42]. In this study, three different ILs have been tested for dissolving and blending chitin/silk with an upper (80%) and lower

(20%) silk content we used: 1-allyl-3-methylimidazoliumchloride (AMIMCl), 1-ethyl-3-methylimidazoliumchloride (EMIMCl), and 1-ethyl-3-methylimidazolium acetate (EMIMAc). AMIMCl and EMIMCl share the same anion chloride but differ in cations, whereas EMIMAc has a distinctive anion acetate. Understanding the modification of the regenerated blended chitin/silk structure based on their various ILs has not been fully studied yet. Our investigation focuses on comparing the stability and structural modification of chitin/silk based as a function of different IL types, and on comparing the structural variation behavior of each IL on the film as the amount of silk content increases from 20% to 80%. The regenerated films were characterized using Fourier Transform Infrared spectroscopy (FTIR), Thermogravimetric analysis (TGA), Scanning Electron Microscope (SEM) and Differential Scanning Calorimetry (DSC) techniques.

## Material and Methods

### Material

Chitin from shrimp shells was purchased from Sigma (C7170). The silk protein was provided by Dr. Xiao Hu from Rowan University. Ionic liquids AMIMCl, EMIMCl and EMIMAc were all purchased from Alfa Aesar.

### Experiment

AMIMCl, EMIMCl and EMIMAc were placed separately in a test tube (representing 95 w/w of the total weight). Then the tube was placed on a hotplate. α-Chitin and silk fibroin were added (representing 5 w/w of the total weight), and the experiment was run between 100-105 ℃ for 48 hours using magnetic stirring. The blended films were transferred between two glass slides. Water was added to the films to

regenerate the chitin/silk films and the samples were kept in water for another 48 hours to remove as much IL as possible at 25℃. The films were dried for 24 hours in a vacuum oven at 50℃.

**Characterization Methods**

Attenuated Total Reflectance Fourier Transform Infrared spectroscopy (ATR-FTIR )

Fourier transform infrared Spectra (FTIR) analysis was performed using Bruker's ALPHA-Platinum FTIR Spectrometer, with Platinum-Diamond sample module and Bruker OPUS Mentor Plus software version 7.2, Build: 7.2.139.1294. The spectra were collected between the wavenumber between 400-4000 $cm^{-1}$, resolution 4 $cm^{-1}$, 32 sample scans and 128 background scans. Six different locations were analyzed for each sample and averaged together. The percentage of the crystallinity of beta sheet of silk were obtained from each sample by selecting the Fourier Self Deconvolution, and the frequency range was set between 1700-1500 $cm^{-1}$ to enable the spectrum to be interactive in that wavenumber [50]. Then parameters were set as the following: Noise reduction 0.30, Bandwidth 25 with Lorentzian. Local Least Square and Gauss shape methods. To obtain the crystallinity of beta sheet, the sum numbers of beta sheet were divided by the sum numbers of the integral.

Thermogravimetric analysis (TGA)

Thermal data was obtained using Thermogravimetric Analysis (TGA) which was carried out on TA Instruments Discovery system, performed on all samples in a nitrogen atmosphere. The heat process was run from 10 ℃/min ramp up to 650 ℃ for average

sample of 6mg. The software determines derivative plot by using the peak height analysis. Differential Scanning Calorimetry (DSC)

Samples (approximately 5mg) were enclosed in TZero aluminum pans and run in a TA Instruments Discovery with a Refrigerated cooling system (RCS) with nitrogen gas flow (25 mL $min^{-1}$). The standard Aluminum reference was used to calibrate the heat capacity. Samples heated from 5 ℃/min to 120 ℃ to allow the water to evaporate. They were then cooled down to -30 ℃, and heated up again to 170 ℃.

Scanning Electron Microscope (SEM)

The SEM images were taken on the LEO1450EP SEM at Rutgers University Camden campus. A small piece was mounted on carbon tape on Denton Desk II Au-Pd sputter coater. The samples were sputter-coated and run in a light-vacuum of 10V for 60 seconds. The magnification used in this paper is with a scale bar of 2000x (10.00μm).

## Results and Discussion

### ATR-FTIR Spectroscopy Analysis

The regenerated chitin/silk films were dissolved with various ILs with different cation and anion species and were coagulated with water at room temperature. The dissolution of chitin in different ILs has been studied previously, and amongst the ILs we used, it has been proven that EMIMAc has the highest proportion of chitin dissolution [62]. As a result, the EMIMAc blended films can be physically characterized as molded solids, while AMIMCl and EMIMCl blended films were unshaped and powdery. The

qualitative results show that the films which have the same anion chloride ILs (EMIMCl and AMIMCl) produce unshaped soft films, while changing the anion size of IL from chloride to acetate (EMIMAc) makes the films more molded and sturdy. This indicates that the extensive hydrogen bonding network in chitin was disrupted further by EMIMAc and created new strong hydrogen bonding between the anion acetate and hydroxyl groups of the chitin [34], amine and carboxyl groups of silk. The following characterization methods allow for further understanding.

To compare the structural modification of chitin/silk films based on different ILs, it is preferable to briefly mention the main functional groups in the pure samples. As observed in Figure 10, chitin spectrum's major peaks are located at OH and NH regions at wavenumber 3600-3200 $cm^{-1}$, amide I (1629 and 1662 $cm^{-1}$), II (1558 $cm^{-1}$) and III (1312 $cm^{-1}$) regions, and C-O-C bond at 1045 $cm^{-1}$. Silk fibroin spectrum shares the presence of NH, amide I, II and III with chitin at wavenumber 3285, 1623, 1517, 1233 $cm^{-1}$ respectively. ILs have common C-H peaks which are located around 3000-2800 $cm^{-1}$, C=C (imidazolium ring) peaks at 1560 $cm^{-1}$ and CN peaks at 1150 $cm^{-1}$. In EMIMAc, there is a unique sharp peak at 1376 $cm^{-1}$ wavenumber which corresponds to the anion species (C−C bond in the anion).

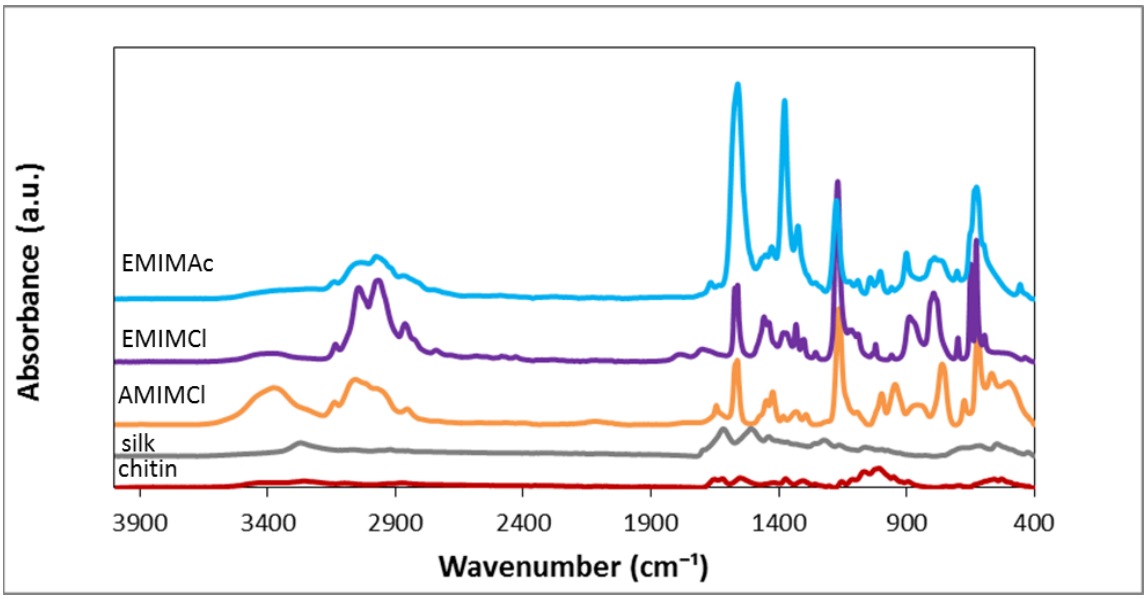


**Figure 10.** The IR spectra for pure ILs, EMIMAc, EMIMCl, AMIMCl and pure chitin and silk component

FTIR spectra of chitin/silk blended materials are assessed based on ILs and the silk compositions. Figure 11 allows the comparison of chitin/silk IL films to be constructed. Various ILs have shown different impacts on the overall blended structures. In all IL films, similar peaks appear for OH, amide I, II, III, COC and C-C bond regions. In addition, the CN (aromatic ring) peak is found in all IL films. Generally, the EMIMAc films spectra are distinguishable from EMIMCl and AMIMCl films spectra mostly between 1690-1300 $cm^{-1}$ region, while the IR of AMIMCl and EMIMCl blended films display similar spectra. Thus, EMIMAc films have the most altered structure (compared to the pure chitin in Figure 10), especially in the bonds that are located in the 1690-1300 $cm^{-1}$ region. The peak at 1550 $cm^{-1}$, which is related to the amide II bond and CO stretching of the acetyl group (overlapping of two acetyl groups of IL and pure chitin), is

more intense and broad than in the EMIMCl and AMIMCl films, and there is no significant difference in this region between EMIMCl and AMIMCl films. Furthermore, EMIMAc films have a single sharp peak at 1690 $cm^{-1}$ (amide I), compared with other IL films that have two peaks (1655-1625 $cm^{-1}$), which is very similar to the pure chitin spectrum [63]. Another notable difference between chloride and acetate films in IR is in 1440-1350 $cm^{-1}$ region (asymmetrical CH bending of the $CH_2$ group [51]). That peak is split into two peaks and became more intense. Also, amide III region (around 1300 $cm^{-1}$), is shifting to the higher wavenumber in EMIMAc films. These modifications of the structure in EMIMAc films may indicate that the interaction increases between hydroxyl group and acetyl groups of chitin and anion species (acetate), and that possible amide of silk causes the structural changes observed in IR spectrum altering of the pure chitin.

In this study, we also looked at the chitin/silk structural modification as the concentration of silk increases from 20% to 80%. Initially, we assumed that the interaction between silk and chitin increases when the concentration of silk increases. As can be seen in Figure 11, there are no remarkable changes between 20% and 80% silk in all three IL films. Yet, the crystallinity of beta sheet calculation, using Local Least Square and Gauss shape methods [50], indicates enhancement in crystallinity as amount of silk added in all blended films. Table 4 shows the percentage of crystallinity of beta sheet in 20% and 80% silk of IL films. In the EMIMAc films (EMIMAc/S20 to EMIMAc/S80), the percent crystallinity increased from 37.2% to 44.8%, from 22.4% to 42.2% in AMIMCl films (AMIMCl/S20 to AMIMCl/S80), and from 27.5% to 39.6% in EMIMCl films (EMIMCl/S20 to EMIMCl/S80). This could indicate structural

modification as the silk ratio changed, causing the interaction that made the crystallinity of beta sheet to be higher in all IL films. The larger amount of silk (80%) might be enough to create extra hydrogen bonding with chitin monomers, and the swollen beta sheet of silk that may not find enough amount of chitin chains to interact with. This could cause the beta sheets to self-assemble which increases the crystallinity.

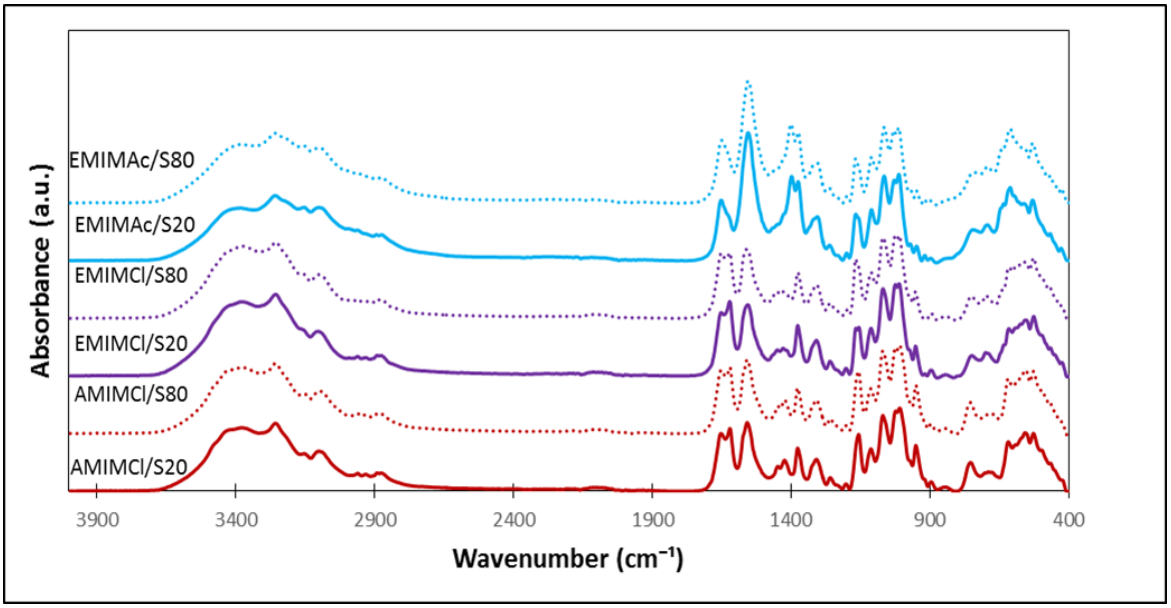


**Figure 11.** The FTIR spectra of regenerated blended films, chitin/silk20 AMIMCl (AMIMCl/S20), chitin/silk80 AMIMCl (AMIMCl/silk80), chitin/silk20 EMIMCl (EMIMCl/S20), chitin/silk80 EMIMCl (EMIMCl/S80), chitin/silk20 EMIMAc (EMIMAc/S20), chitin/silk80 EMIMAc (EMIMAc/S80).

| Sample | Crystallinity of beta sheet |
|---|---|
| EMIMAc/S20 | 37.2% |
| EMIMAc/S80 | 44.8% |
| AMIMCl/S20 | 22.4% |
| AMIMCl/S80 | 42.2% |
| EMIMCl/S20 | 27.5% |
| EMIMCl/S80 | 39.6% |

**Table 4.** The crystallinity of beta sheet at 20% and 80% silk films

**Morphology Analysis (SEM)**

The surfaces of ILs chitin/silk films were studied using scanning electron microscopy (SEM) to contrast the morphological properties of the various IL films. The images illustrate notable changes according the type of cation, anion or silk proportion. Looking at the three images on the left side of Figure 12, the IL films that have the same cation species with an ethyl functional group (EMIMCl and EMIMAc) show rough surfaces, while the film containing an allyl group (AMIMCl) reveals some divided parts (cuts) in its morphology. Moreover, a fibrous structure is observed in the surface of the ethyl films (EMIMAc/S20 and EMIMCl/S20). This possibly contributes to the interaction that ethyl caused within the structure possibly resulting in similar topology for EMIMCl and EMIMAc films. The films with high elevated silk content have smoother topology in all IL films [34], which probably indicates increases in the interaction between the

hydroxyl function of chitin with amine and the hydroxyl function of silk, as seen in the calculation of crystallinity of beta sheet, and the dominance of the silk structure.

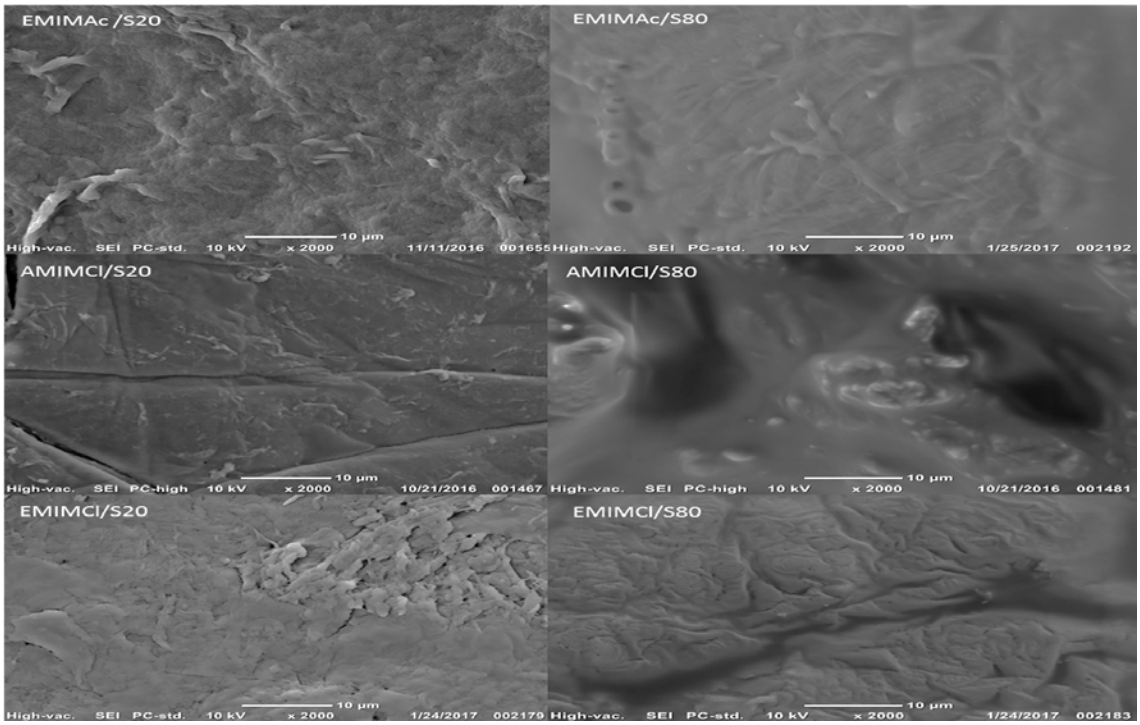


**Figure 12.** The SEM images of IL films of chitin/silk for AMIMCl, EMIMCl and EMIMAc at 20% and 80% silk

**Thermal Analysis (TGA)**

The thermal stability of the blended films was assessed by thermogravimetric analysis to determine the thermal behavior of chitin based on the different ILs used and silk composition. Thermogravimetric analysis results of the chitin/silk IL films are given in Figure 13. Generally, the thermal stability of the samples is controlled based on the type of IL used to regenerate the sample [36]. The initial weight loss around 100℃ is due

to the loss of moisture [32, 54]. The maximum decomposition, 1 and 2, for the IL films are shown in Table 5. EMIMAc films show less thermal stability compared with other IL films. This can lead the comparison to be made based on the anion type, which means that the films that have the acetate anion are less thermally stable even though they perform superior mixture films relative to EMIMCl and AMMICl [34, 62]. Alternatively, the EMIMCl films acquire the highest thermal stability. Yet, the EMIMAc/S20 illustrates the second minor decomposition over 350 ℃, which has high thermal stability in that position. Changing the size of anion from small ion chloride to bigger ion acetate can decrease thermal stability due to the increase in the backbone spacing between the chitin and silk, and due to an increase in number of interactions. Despite the fact that AMIMCl and EMIMAc share no characteristics in either cation or anion domains, the observation of the late peak (decomposition 2) over 350 ℃ was seen in both EMIMAc/S20 and AMIMCl/S20 films. The lowest early decomposition peak (1) appears around 203 ℃ in EMIMCl/S20, whereas it does not appear in other ILs. Moreover, a broad derivative range between 200-350 ℃ is noticed in EMIMCl/S20 which is similar to the pure chitin line decomposition (Figure 13). Possibly EMIMCl have less effect on chitin chains while EMIMAc and AMIMCl have the ability to disrupt some chitin chains by functionalizing some acetamido groups and allowing to interact with beta sheet of silk. The low maximum temperature decomposition shown in AMIMCl/S20 and EMIMAc/S20 samples may be related to the functionalized acetamido backbone (the first phase) and the second phase may be related to the un-functionalized acetamido backbone [64].

In addition to the comparison of different ILs used, the thermal stability as a function of increasing the silk content in each individual IL films was also evaluated. As

the concentration of protein increases (20% to 80%) the AMIMCl samples follow the rule for slightly increasing the decomposition temperature (as seen in chapter 2) [32]. This might be responsible for the increase in the interaction between silk and chitin chains with control of the allyl function for stability rearranging. The allyl group of AMIMCl which contains a double bond, seems more reactive than groups without a double bond; thus, this increasing of thermal stability from AMIMCl/S20 to AMIMCl/S80 was expected [62]. Conversely, the EMIMAc and EMIMCl samples show no significant change. In 80% silk samples, all IL films display one step decomposition due to being composed predominately of silk.

| **Sample** | **Maximum decomposition (1)℃** | **Maximum decomposition (2)℃** |
|---|---|---|
| chitin | 287 | 396 |
| silk | 322 | - |
| EMIMAc/S20 | 242 | 383 |
| EMIMAc/S80 | 240 | - |
| EMIMCl/S20 | 203 | 275 |
| EMIMCl/S80 | 295 | - |
| AMIMCl/S20 | 254 | 380 |
| AMIMCl/S80 | 285 | - |

**Table 5.** The maximum decomposition temperatures (1, 2) for pure chitin, silk and regenerated chitin/silk IL films

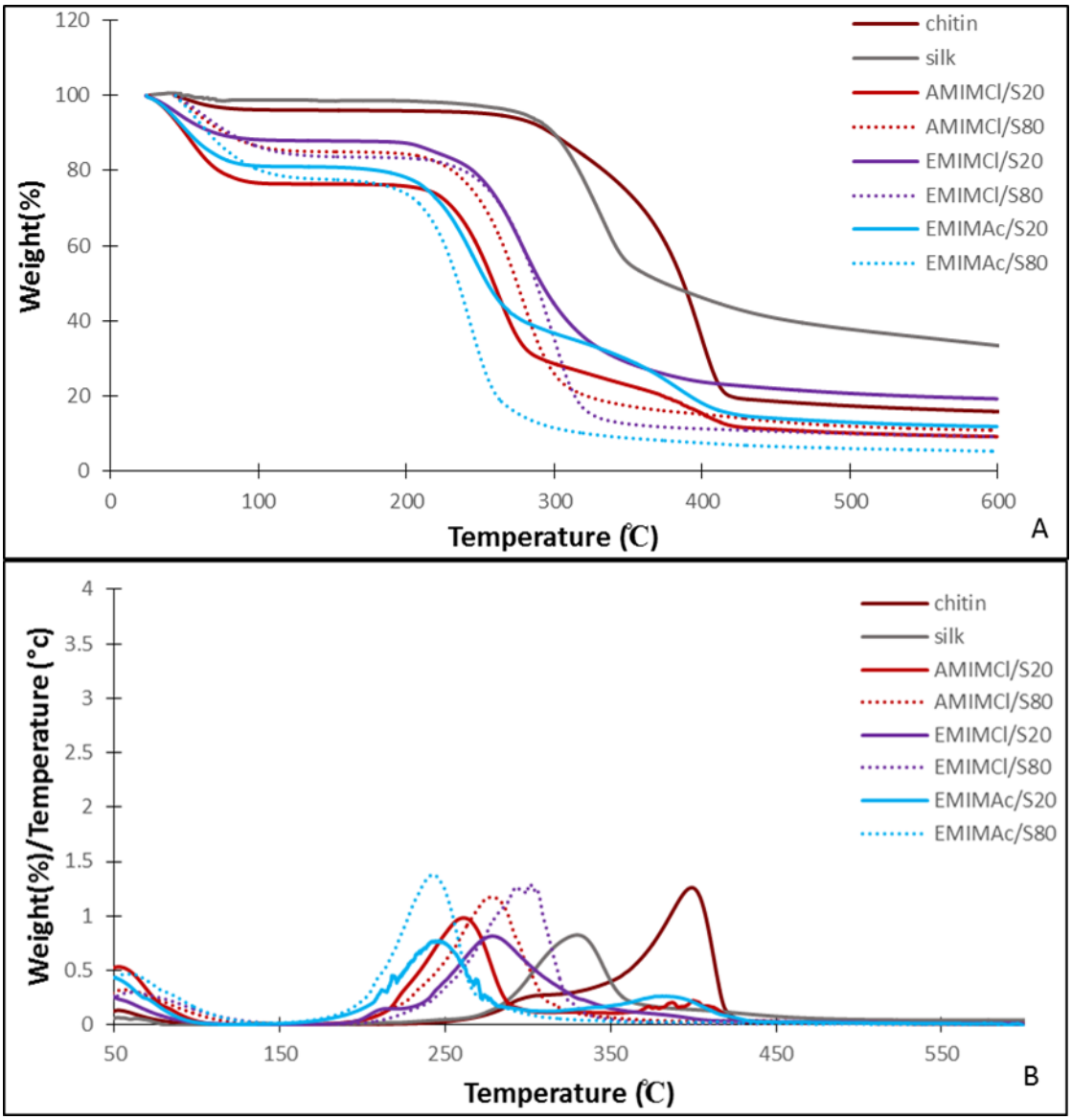


**Figure 13.** The thermal degradation of pure chitin, silk and regenerated chitin/silk sample with ILs. A) percent weight decomposition B) derivative percent weight decomposition

Now we discuss the thermal degradation of chitin films 100% chitin/ILs (no silk in the films) to show that the two decomposition temperatures are also found in the pure films, and they varied depending on the type of ILs used. As seen in Figure 14, all three IL films have two degradation steps. However, the AMIMCl and EMIMAc films illustrate about 50:50 degradation of the films, while EMIMCl film shows unequal degradation. This possibly indicates that the films containing AMIMCl and EMIMAc have more space between chitin backbone which means that these ILs have somehow the ability to disrupt some of the inter-molecular interaction between chitin chains resulting in increasing the space between chitin backbone, and the thermal degradation shows two steps. In addition, the thermal graph shows low temperature degradation for chains that are perturbed by AMIMCl and EMIMAc while higher degradation temperature for the chains not effected by ILs. It could also be related to the regenerating process which causes these chains to come tightly together resulting in an increase in their degradation temperature. On the other hand, EMIMCl film has less spacing between chains which indicates that EMIMCl has less disrupting ability and less phase separation. Overall, from the thermal graphs, we can infer that the two degradation temperatures are mainly related to the chitin morphology and its ability for the chains disentanglement in ionic liquid and/ or during their reassembly in water.

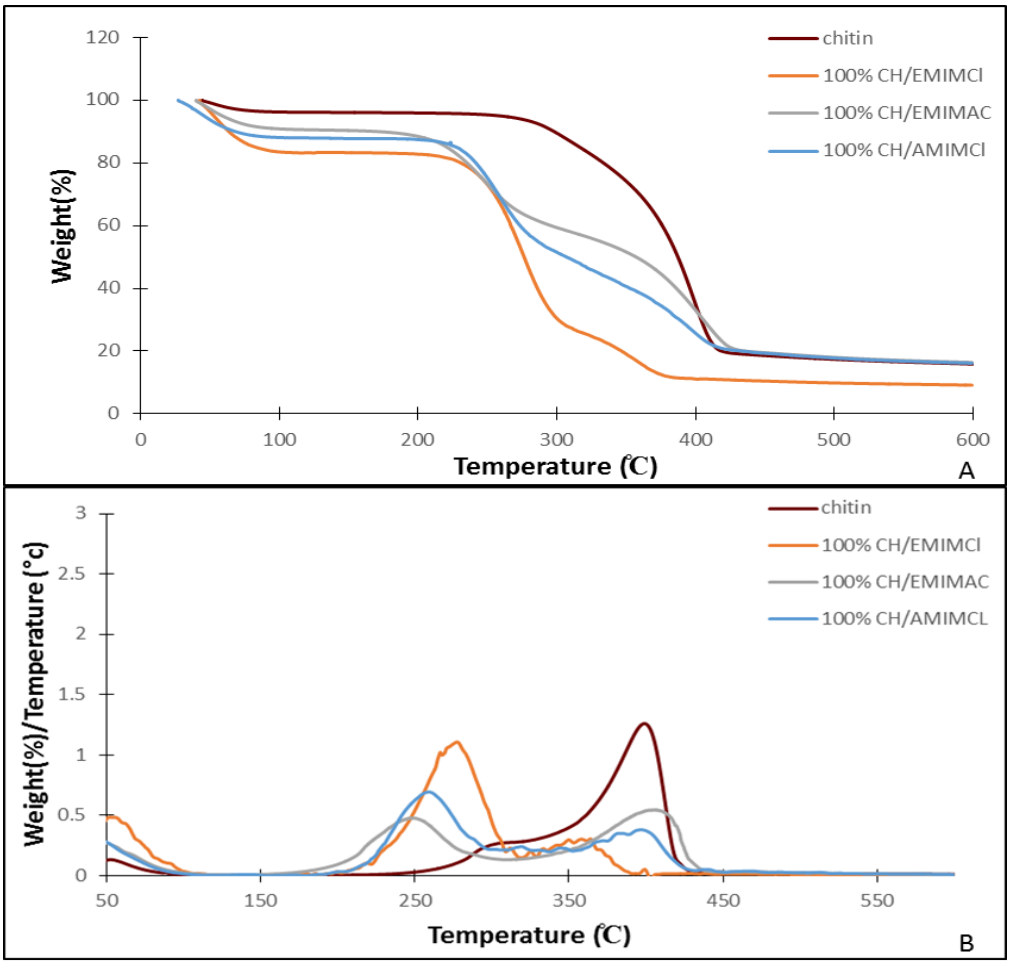


**Figure 14.** Thermal degradation for pure chitin and 100% chitin film in three different ILs, A) percent weight decomposition B), derivative percent weight decomposition

**Thermal Analysis (DSC)**

Figure 15 illustrates the DSC thermogram curves for blended chitin/silk IL films. According to the ILs utilized, the EMIMAc films display the obvious broad water evaporation ($T_w$) peak in range of 70-160 ℃. In contrast to the EMIMAc films, it is hard to observe the $T_w$ peak in the EMIMCl/S20 line. The AMIMCl samples have the water evaporation peak between 90-130 ℃. From this result, we could say that the EMIMAc

films absorb more water than EMIMCl and AMIMCl films, while EMIMCl/S20 has less ability to absorb water. Let's remember that the thermograms showed in Figure 15 shows the 2$^{nd}$ cycle results after evaporating most of the water during the first cycle; hence, $T_w$ can be related to the glass transition temperature. The glass transition temperature $T_g$, for pure silk is around 180℃ and for pure chitin is around 130℃ [56, 57]. Also, it has been reported that the $T_g$ decreases as the water content increases for chitin. Thus, the increase in $T_w$ of our biomaterials is related to both a decrease in water content and an increase in silk content, specially an increase in beta sheet formation. In addition, the number of interactions of acetate anions can play a significant role in this observation. The TGA analysis demonstrated that EMIMCl/ S20 has greater thermal stability while EMIMAc has the lowest. As the silk content increases, the $T_w$ peak is similar in the AMIMCl/S80 sample (going from AMIMCl/S20 to AMIMCl/S80), which correlates to the thermal stability as seen in TGA analysis. Alternatively, $T_w$ increases as the silk content increases as in EMIMAc (EMIMAc/S20 to EMIMAc/S80) samples. As mentioned earlier, this is related to an increase in amount of interaction and due to an increase in silk content. Pure silk has a higher $T_g$ than pure chitin. This is consistent with previous results [36]. DSC analysis indicates a strong relationship to water content and an increased number of interactions.

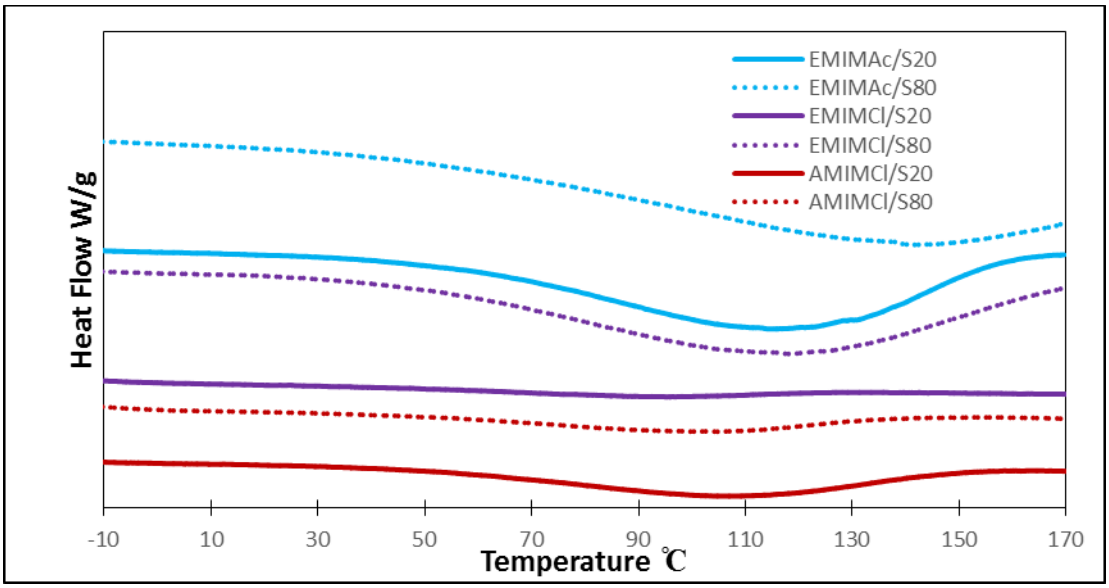


**Figure 15.** DSC curves of blended chitin/silk IL films at 20% and 80% silk concentration

**Conclusion**

In this study, we compared the behavior of blended chitin/silk (at 20% and 80% silk) films in three different types of ILs: AMIMCl, EMIMCl and EMIMAc. We observed the modification of the structural, morphological, and thermal properties according to their variances in anion and cation species of ILs, as well as the silk composition. The films that contain the same anion chloride (EMIMCl and AMIMCl films) performed similarly in the IR spectrum (very similar to the pure chitin spectrum), while the acetate anion (EMIMAc films) has a unique spectrum (different than the pure chitin spectrum). The thermal degradation for acetate films has the lowest stability, yet in the (EMIMAc/S20) film, there is a minor degradation peak (second degradation) over 350℃. In the 100 % chitin films, the two degradation temperatures are mainly related to the chitin morphology and its ability for the chain to disentangle in ionic liquid and reassemble in water. The EMIMCl films show the highest thermal stability amongst the

IL films. The size and number of interactions of the anion can play a role in thermal stability, as the size of the anion increases, the thermal stability decreases. The increase of the silk content promotes the increase of the crystallinity of the beta sheet in all prepared films. In addition, the increase of the silk concentration impacts thermal stability. In the AMIMCl and EMIMCl films, the thermal stability was slightly enhanced as the silk increased. This enhancement was not observed with the film regenerated with EMIMAc. In DSC analysis, the broad range in $T_w$ appeared in the EMIMAc films and EMIMCl/S80. Alternatively, the lowest observed peak is shown in EMIMCl/S20, which has the higher thermal stability in TGA analysis. In the SEM analysis, it seems that the type of cation plays a small role in controlling the overall surface of the blended films. The surface of the sample that include the ethyl cation displayed the fibrous structural surface (EMIMAc and EMIMCl films). By understanding the effect of each IL on blending chitin with silk using upper and lower ratios of silk, the design of tissue engineering scaffolds can be controlled.

**Abbreviation: chitin/silk 20 AMIMCl (AMIMCl/S20), chitin/silk 80 AMIMCl (AMIMCl/S80), chitin/silk 20 EMIMCl (EMIMCl/S20), chitin/silk 80 EMIMCl (EMIMCl/S80), chitin/silk 20 EMIMAc (EMIMAc/S20), chitin/silk 80 EMIMAc ( EMIMAc/S80)**

## Chapter 4: Study of Blending Chitosan/Silk in AMIMCl and EMIMCl

Chitosan is an important derivative of chitin, and chitin has been converted to chitosan to improve its processing strategies [20]. Blended systems of chitosan with silk have shown considerable potential for skin-healing applications [29, 34, 45]. Ionic liquids have been studied as a solvent to dissolve chitosan with silk, yet the structural modifications and thermal stability of regenerated IL materials have not been fully explored in the literature. In this brief study, chitosan/ silk materials have been blended using two different ionic liquids as a solvent, [AMIMCl] (1-allyl-3-methylimidazolium chloride), [EMIMCl] (1-ethyl-3-methylimidazolium chloride) with 20% and 80% silk concentration. Here the modifications of structure are seen in FTIR, DSC, TGA and SEM (Figures 16-19).

The films' preparation is described in Chapters 2 and 3. Figure 16 shows the IR spectrum of chitosan/silk IL films. The main observed difference between AMIMCl and EMIMCl films is in the range of 1700-1000 $cm^{-1}$. At wavenumber 1458 $cm^{-1}$, the peak is split into two peaks and became more intense in AMIMCl films in comparison with EMIMCl films. Looking for the comparison based on the increase of silk content (from 20% to 80% silk) in these IL films, the IR spectra show no significant difference between 20% and 80% silk samples. Yet, the crystallinity of beta sheet displays an increase as silk concentration increases in both AMIMCl and EMIMCl films (Table 6).

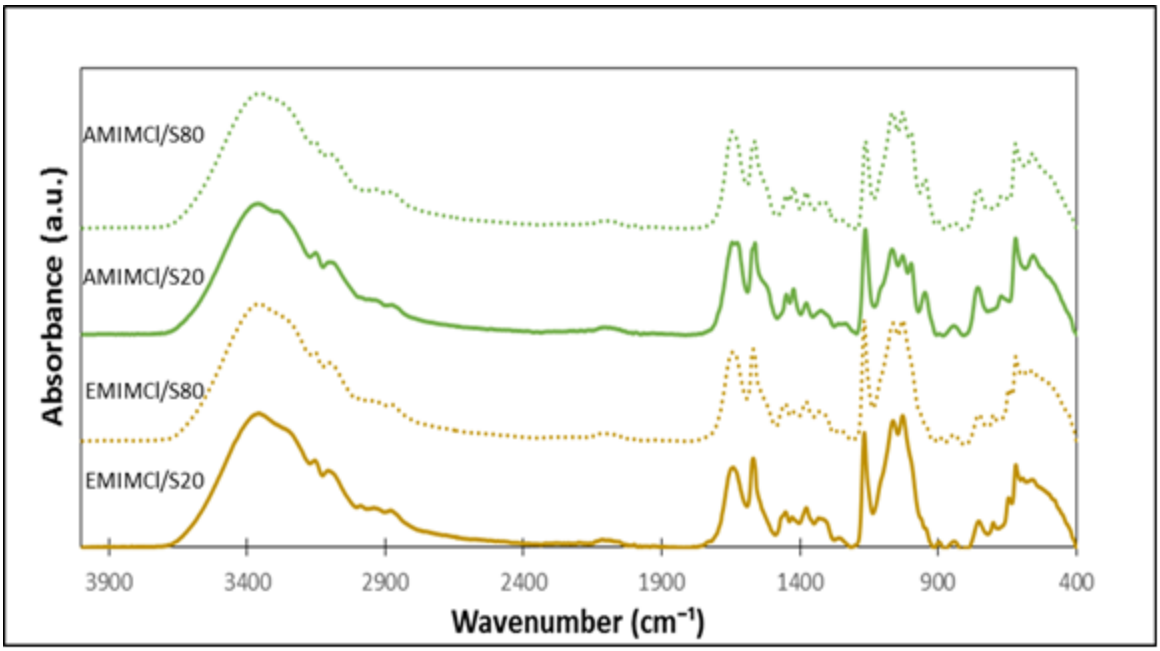


**Figure 16.** The IR spectrum of chitosan/silk IL samples

| Sample | Crystallinity of beta sheet |
|---|---|
| AMIMCl /S20 | 18.1% |
| AMIMCl/S80 | 31.3% |
| EMIMCl/S20 | 28.9% |
| EMIMCl/S80 | 38.4% |

**Table 6.** The crystallinity of beta sheet for chitosan/silk IL films

Figure 17 illustrates thermal analysis for regenerated chitosan/silk IL samples. Both IL films show the early shoulder degradation peak which may relate to the free amine groups in chitosan with amide group of silk weakly interacting during degradation. In AMIMCl films, increases in the silk content (20% to 80% silk) slightly increases the temperature of thermal degradation, indicating that silk content provides thermal stability in the blended films which agrees with the previous study [32]. This result corresponds with an increase in crystallinity of beta sheet in IR analysis. However, EMIMCl films show no effect in thermal degradation as percent silk increases.

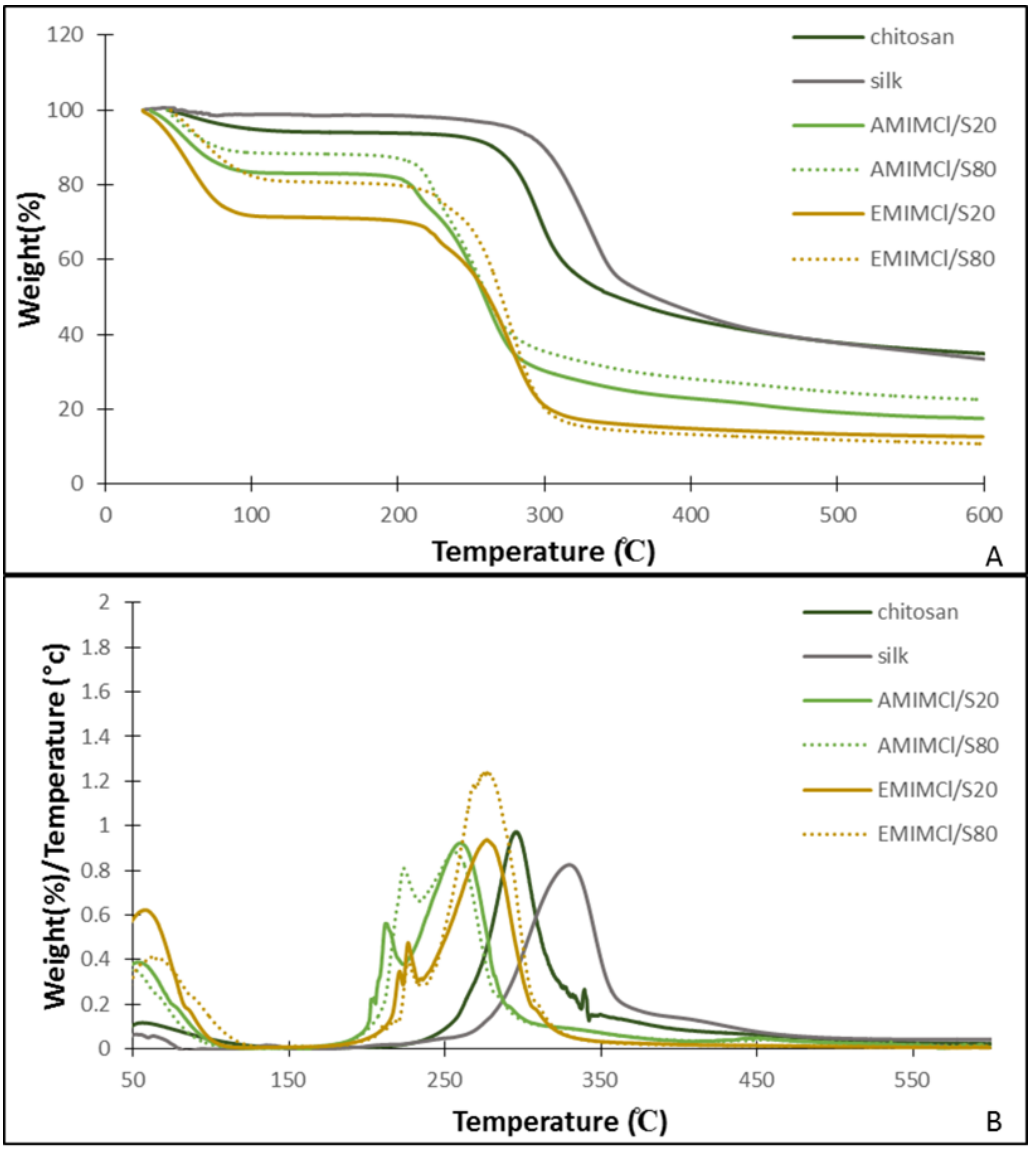


**Figure 17.** The thermal degradation of the pure chitosan, silk and IL films at 20% and 80% silk, A) percent weight decomposition B), derivative percent weight decomposition

The SEM images demonstrate the changes in the films' morphology based on ILs used and silk composition. The films with greater amounts of silk (80% silk) have smoother surfaces than films with less silk (20% silk) in both IL films due to the dominated silk structure (Figure 18). This also, maybe reflecting an increase in the interaction between silk and chitosan as the silk ratio increases, which creates stable

materials as seen in TGA analysis curves. Moreover, the difference can be based on diversity of ILs; EMIMCl/S20 surface film shows less porosity compared with AMIMCl/S20 film.

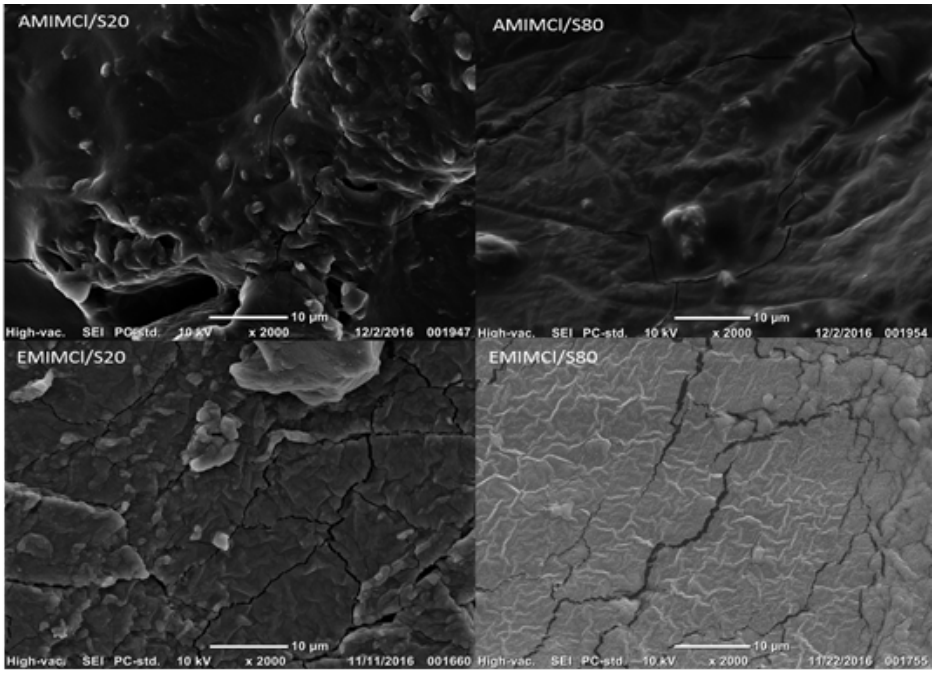


**Figure 18.** SEM images for chitosan/ silk IL films (20%, 80% silk)

The DSC curves for blended materials are shown in Figure 19. The Tg temperature is shifted to higher temperatures in EMIMCl/S80 (as silk amount rose from 20% to 80%), while in AMIMCl /S80 the shifting is not observed.

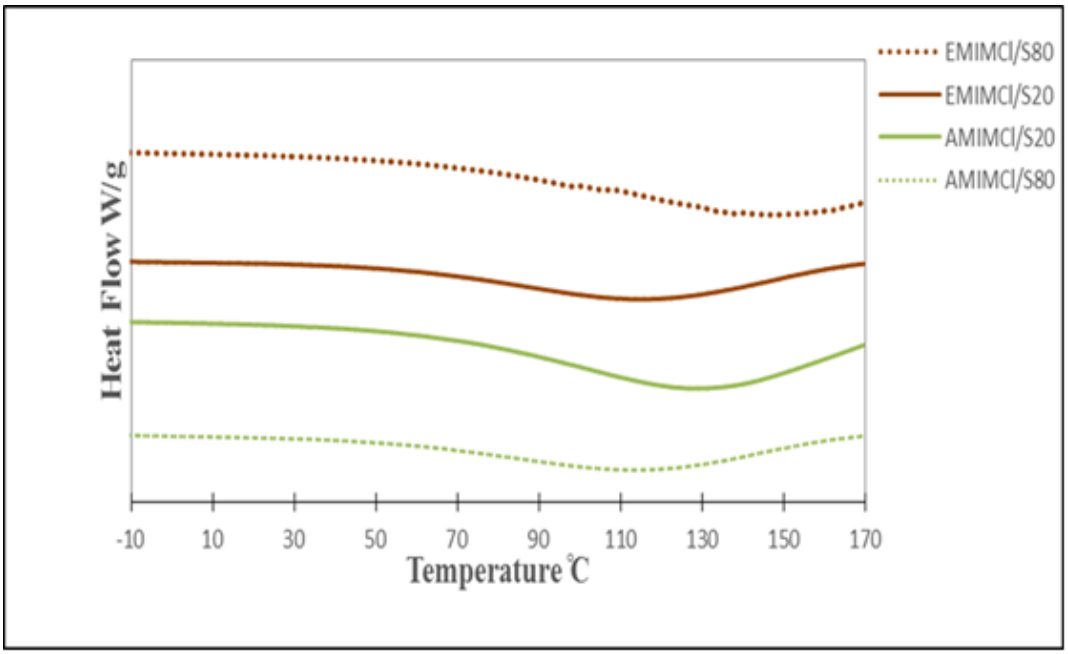


**Figure 19.** DSC curves of chitosan/silk IL films

We also tried to dissolve and blend chitosan/silk in EMIMAc, but we could not regenerate the material using this IL. It has been reported in previous studies that chitosan is not soluble in EMIMAc [65], but our result is somewhat different because our chitosan had been mixed with silk. We observed complete dissolution of chitosan and silk in EMIMAc, and it seems that chains of chitosan and silk could not rearrange again when EMIMAc was used. This means the silk and chitosan chains converted to an amorphous form.

## Conclusion

The calculation of crystallinity of beta sheet provided evidence to suggest that there is a structural modification as the silk ratio increases, which raises the percentage of

crystallinity as calculated by the IR Fourier Self-Deconvolution spectra of beta sheet (1700-1500 $cm^{-1}$). This is also shown in the TGA curves, where the thermal stability slightly increases when the concentration of silk increases in AMIMCl films (AMIMCl/S20 to AMIMCl/S80), while EMIMCl films show no effect in thermal degradation as silk percent increases. In DSC curves, the Tg temperature is shifted to higher temperatures in EMIMCl/S80 (as silk amount rose from 20% to 80%), while in AMIMCl /S80 the shifting is not observed.

**Abbreviation: chitosan/silk 20 AMIMCl (AMIMCl/S20), chitosan/silk 80 AMIMCl (AMIMCl/S80), chitosan/silk 20 EMIMCl (EMIMCl/S20), chitosan/silk 80 EMIMCl (EMIMCl/S80),**

## Chapter 5: Summary

Blended biomaterial (cellulose, chitin, chitosan, silk) systems have been widely studied to obtain desirable properties of the two polymers. In our study, we tried to mimic the complex hierarchical structure of some stable natural structures, such as shrimp shells and cell walls of plants to acquire a stable material that can be used in biomedical applications, specifically in tissue replacement. Non-toxicity, biocompatibility and accessibility of these natural materials make these polymers suitable for medical applications. Moreover, ionic liquids are green solvents with less hazardous and more environmentally friendly sources.

Chapter 2 compared polysaccharide/silk blends (cellulose/silk, chitin/silk, chitosan/silk) based on the different polysaccharides used, and on the increasing amount of silk in each film prepared using AMIMCl solvent. The regenerated films were characterized using FTIR, TGA, DSC and SEM techniques. The regenerated films varied: cellulose/silk films were shaped firm and solid, while chitin/silk and chitosan/silk films were shapeless and powdery. The IR spectra show absorbance increases in the amide I, II bond region as silk proportions increase, regardless of polysaccharide component. As the amount of silk increases from 20% to 80%, the crystallinity of the beta sheet elevates by 9.2 %, 19.8% in chitin-silk films, and an intermediate percentage of 13.2% in chitosan-silk films. This pattern of crystallinity could indicate a higher likelihood of interactions between chitin chains and silk fibers than cellulose and chitosan because of the acetamido functional group in chitin that makes extra hydrogen bonds with silk chains. Also, more amount of silk (80%) might be enough to create extra hydrogen bonding with chains

monomers, and the swollen beta sheet of silk that did not find enough amount of chains to interact with, results in beta sheet self-assembly that increase the crystallinity of beta sheet. TGA results proved that chitin/silk films have greater changes in thermal degradation temperature as the silk ratio grows. In line with the thermal results, the chitosan film (20% silk) had more pores surface in the SEM image than the other polysaccharide films, with this morphology profile possibly correlating to low thermal stability and high water absorbency.

Chapter 3 compared blended chitin/silk films in three different ionic liquids (AMIMCl, EMIMCl, EMIMAc). EMIMAc blended films can be physically characterized as molded solids, while AMIMCl and EMIMCl blended films were shapeless and powdery. The FTIR results showed the regenerated films that contain the same anion chloride (EMIMCl and AMIMCl films) performed similarly in the IR spectrum, especially in the range of 1690-1300 $cm^{-1}$ (very similar to the pure chitin spectrum), while the acetate anion (EMIMAc films) had a unique spectrum (different than the pure chitin spectrum). There is no significant change in FTIR spectrum between 20% and 80% silk films in all ILs. However, the calculation of the crystallinity of beta sheet showed an increase as the silk ratio increased in all IL films. In TGA analysis, the EMIMCl regenerated films had the higher thermal degradation, while EMIMAc films had the lowest thermal stability. Interestingly, the late peak (decomposition 2) over 350 ℃ was seen in both EMIMAc/S20 and AMIMCl/S20 films. This possibly explained that the EMIMCl have less effect on chitin chains while EMIMAc and AMIMCl have the ability to disrupt some chitin chains by functionalizing some acetamide groups and allowing to interact with beta sheet of silk. The two decomposition steps shown in AMIMCl/S20 and

EMIMAc/S20 samples may be related to the functionalized acetamide backbone (the first phase) and the second step may be related to the un-functionalized acetamido backbone.

In chapter 4, we studied blended chitosan/silk in EMIMCl and AMIMCl. The thermal degradation shows an early decomposition present in both IL films. This possibly relates to the free amine groups in chitosan with amide groups of silk weakly interacting during degradation.

**Future Study**

Future study could be performed by increasing the concentration of biomaterials in ILs, and the introduction of ethanol as the coagulating agent to remove the ILs from films. The IR spectra for regenerated films displayed peaks that related to the IL, which means that the IL was not removed completely from the samples. In order to remove the IL, Soxhlet extraction with carbon dioxide/ethanol can be used a repeated cycle times over days [66]. Commonly, a Soxhlet extraction is utilized when the compound has limited solubility in a solvent, as in our case. In this way, the temperature can be controlled during the IL removal. X-ray and Nuclear magnetic resonance spectroscopy (NMR) analysis are needed for further structural modification.

Although ILs are considered green solvents, some studies showed a certain level of toxicity was exhibited in commonly used ILs, so some bio tests such as cytoxicity, cell behavior, antimicrobial assessments and enzymatic biodegradation are needed [27, 33, 66, 67]. Fabricated materials may be potential candidates for several biomedical applications, including tissue engineering. For such applications, then, cytotoxicity assays should be considered for future study [49, 68].

ILs that have the larger anion might play a role in disrupting the hydrogen bonds in chitin and chitosan as seen in the previous chapters. Also, changing the cation could contribute to better mixing. For example, the cation can be changed to a larger functional group while keeping the anion size such as 1-butyl-3-methylimidazolium chloride (BMIMCl), or both ions could be changed, such as 1-butyl-3-methylimidazolium bromide (BMIMBr), or 1-butyl-3-methylimidazolium methane sulfonate ($BMIMMeSO_3$).

Other proteins that can be mixed with polysaccharides are collagen, keratine, and gelatin-alginate, which are considered the most popular 3D scaffolds for tissue regeneration [3, 49, 69]. These proteins have an excellent biocompatibility and biodegradability for medical applications. In addition, since keratin is protein found in human hair, keratin can be considered as biomaterials that can be blended with polysaccharides and used in biomedical applications. Lignin, which can be obtained as a waste product of the paper industry, has multifunctional barrier properties and many functional groups, so it can be utilized to increase the binding properties in the blended system [70].

**References**

1. Tathe, A., M. Ghodke, and A.P. Nikalje, A brief review: biomaterials and their application. International Journal of Pharmacy and Pharmaceutical Sciences, 2010. 2(4): p. 19-23.

2. Ratner, B.D., A.S. Hoffman, F.J. Schoen, and J.E. Lemons, Biomaterials science: a multidisciplinary endeavor. Biomaterials science: an introduction to materials in medicine. 2004: Elsevier Academic Press. p. 1-9.

3. Ha, T.L.B., T.M. Quan, D. Vu, D. Si, and J. Andrades, Naturally derived biomaterials: Preparation and application. Regenerative Medicine and Tissue Engineering. 2013: InTech. p. 247-274.

4. Lutolf, M. and J. Hubbell, Synthetic biomaterials as instructive extracellular microenvironments for morphogenesis in tissue engineering. Nature Biotechnology, 2005. 23(1): p. 47-55.

5. Palao-Suay, R., L. Gómez-Mascaraque, M. Aguilar, B. Vázquez-Lasa, and J. San Román, Self-assembling polymer systems for advanced treatment of cancer and inflammation. Progress in Polymer Science, 2016. 53: p. 207-248.

6. Ige, O.O., L.E. Umoru, and S. Aribo, Natural products: A minefield of biomaterials. ISRN Materials Science, 2012. 2012: p. 1-20.

7. El-Hefian, E.A., M.M. Nasef, and A.H. Yahaya, Chitosan-based polymer blends: Current status and applications. Journal of Chemical Society of Pakistan, 2014. 36(1): p. 11-27.

8. Doh, K.-O. and Y. Yeo, Application of polysaccharides for surface modification of nanomedicines. Therapeutic Delivery, 2012. 3(12): p. 1447-1456.

9. Nelson, D.L., A.L. Lehninger, and M.M. Cox, Lehninger principles of biochemistry. 2008: Macmillan. p. 235-270.

10. Singh, R.S., G.K. Saini, and J.F. Kennedy, Pullulan: microbial sources, production and applications. Carbohydrate Polymers, 2008. 73(4): p. 515-531.

11. Lapasin, R. and S. Pricl, Industrial applications of polysaccharides, in Rheology of Industrial Polysaccharides: Theory and Applications (Lapsdin). 1995, Springer Science, US. p. 134-161.

12. Biao, H., C. Xue-rong, D. Da-song, L. Tao, O. Wen, and T. Li-rong, Preparation of Nanocellulose with Cation-Exchange Resin Catalysed Hydrolysis. 2011: INTECH Open Access Publisher. p. 139-152.

13. George, J. and S. Sabapathi, Cellulose nanocrystals: synthesis, functional properties, and applications. Nanotechnology, Science and Applications, 2015. 8: p. 45-54.

14. Krishna, L.N.V., P. Kulkarni, M. Dixit, D. Lavanya, and P.K. Raavi, Brief introduction of natural gums, mucilages and their applications in novel drug delivery systems-A review. International Journal of Drug Formulation and Research, 2011. 2(6): p. 54-71.

15. Kang, H., R. Liu, and Y. Huang, Graft modification of cellulose: Methods, properties and applications. Polymer, 2015. 70: p. A1-A16.

16. Zhou, L., Q. Wang, J. Wen, X. Chen, and Z. Shao, Preparation and characterization of transparent silk fibroin/cellulose blend films. Polymer, 2013. 54(18): p. 5035-5042.

17. Yuan, X. and G. Cheng, From cellulose fibrils to single chains: understanding cellulose dissolution in ionic liquids. Physical Chemistry Chemical Physics, 2015. 17(47): p. 31592-31607.

18. Lewis, A., J.C. Waters, J. Stanton, J. Hess, and D. Salas-de la Cruz, Macromolecular Interactions Control Structural and Thermal Properties of Regenerated Tri-Component Blended Films. International Journal of Molecular Sciences, 2016. 17(12): p. 1989.

19. Rinaudo, M., Chitin and chitosan: Properties and applications. Progress in Polymer Science, 2006. 31(7): p. 603-632.

20. Dutta, P.K., J. Dutta, and V. Tripathi, Chitin and chitosan: Chemistry, properties and applications. Journal of Scientific and Industrial Research, 2004. 63(1): p. 20-31.

21. Chang, C., S. Chen, and L. Zhang, Novel hydrogels prepared via direct dissolution of chitin at low temperature: structure and biocompatibility. Journal of Materials Chemistry, 2011. 21(11): p. 3865-3871.

22. Arbia, W., L. Arbia, L. Adour, and A. Amrane, Chitin extraction from crustacean shells using biological methods-a review. Food Technology and Biotechnology, 2013. 51(1): p. 12-25.

23. Kaya, M., E. Lelešius, R. Nagrockaitė, I. Sargin, G. Arslan, A. Mol, T. Baran, E. Can, and B. Bitim, Differentiations of Chitin Content and Surface Morphologies of Chitins Extracted from Male and Female Grasshopper Species. PLoS ONE, 2015. 10(1): p. e0115531.

24. Jaworska, M.M. and A. Gorak, Modification of chitin particles with chloride ionic liquids. Materials Letters, 2016. 164: p. 341-343.

25. Ivanova, E.P., K. Bazaka, and R.J. Crawford, New Functional Biomaterials for Medicine and Healthcare. Vol. 67. 2014: Woodhead Publishing. p. 32–70.

26. Younes, I. and M. Rinaudo, Chitin and chitosan preparation from marine sources. Structure, properties and applications. Marine Drugs, 2015. 13(3): p. 1133-1174.

27. Sharma, C., A.K. Dinda, P.D. Potdar, and N.C. Mishra, Fabrication of quaternary composite scaffold from silk fibroin, chitosan, gelatin, and alginate for skin regeneration. Journal of Applied Polymer Science, 2015. 132(44): p. 1-12.

28. Jin, J., P. Hassanzadeh, G. Perotto, W. Sun, M.A. Brenckle, D. Kaplan, F.G. Omenetto, and M. Rolandi, A Biomimetic Composite from Solution Self-Assembly of Chitin Nanofibers in a Silk Fibroin Matrix. Advanced Materials, 2013. 25(32): p. 4482-4487.

29. Bhardwaj, N. and S.C. Kundu, Silk fibroin protein and chitosan polyelectrolyte complex porous scaffolds for tissue engineering applications. Carbohydrate Polymers, 2011. 85(2): p. 325-333.

30. Shang, S., L. Zhu, and J. Fan, Physical properties of silk fibroin/cellulose blend films regenerated from the hydrophilic ionic liquid. Carbohydrate Polymers, 2011. 86(2): p. 462-468.

31. Thenmozhi, N., T. Gomathi, and P. Sudha, Preparation and characterization of biocomposites: Chitosan and silk fibroin. Der Pharmacia Lettre, 2013. 5(4): p. 88-97.

32. Moraes, M.A.d., G.M. Nogueira, R.F. Weska, and M.M. Beppu, Preparation and characterization of insoluble silk fibroin/chitosan blend films. Polymers, 2010. 2(4): p. 719-727.

33. Chen, J.-P., S.-H. Chen, and G.-J. Lai, Preparation and characterization of biomimetic silk fibroin/chitosan composite nanofibers by electrospinning for osteoblasts culture. Nanoscale Research Letters, 2012. 7(1): p. 170.

34. Silva, S.S., T.C. Santos, M.T. Cerqueira, A.P. Marques, L.L. Reys, T.H. Silva, S.G. Caridade, J.F. Mano, and R.L. Reis, The use of ionic liquids in the processing of chitosan/silk hydrogels for biomedical applications. Green Chemistry, 2012. 14(5): p. 1463-1470.

35. Jao, D., X. Mou, and X. Hu, Tissue Regeneration: A Silk Road. Journal of Functional Biomaterials, 2016. 7(3): p. E22.

36. Stanton, J., Y. Xue, J.C. Waters, A. Lewis, D. Cowan, X. Hu, and D. Salas-de la Cruz, Structure–property relationships of blended polysaccharide and protein biomaterials in ionic liquid. Cellulose, 2017. 24(4): p. 1775-1789.

37. Swatloski, R.P., S.K. Spear, J.D. Holbrey, and R.D. Rogers, Dissolution of cellose with ionic liquids. Journal of the American Chemical Society, 2002. 124(18): p. 4974-4975.

38. Moroni, A. and T. Havard, Characterization of polyesters and polyamides through SEC and light scattering using 1, 1, 1, 3, 3, 3-hexafluoro-2-propanol as eluent. Polymeric Materials Science and Engineering(USA), 1997. 77: p. 14-16.

39. Kadokawa, J.-I., Ionic liquid as useful media for dissolution, derivatization, and nanomaterial processing of chitin. Green and Sustainable Chemistry, 2013. 3(2A): p. 19-25.

40. Xie, H., S. Zhang, and S. Li, Chitin and chitosan dissolved in ionic liquids as reversible sorbents of CO2. Green Chemistry, 2006. 8(7): p. 630-633.

41. Ghandi, K., A review of ionic liquids, their limits and applications. Green and Sustainable Chemistry, 2014. 2014: p. 44-53.

42. Mallakpour, S. and M. Dinari, Ionic liquids as green solvents: progress and prospects, in Green Solvents II. 2012, Springer. p. 1-32.

43. Wegst, U.G., H. Bai, E. Saiz, A.P. Tomsia, and R.O. Ritchie, Bioinspired structural materials. Nature Materials, 2015. 14(1): p. 23-36.

44. Yong, S.K., M. Shrivastava, P. Srivastava, A. Kunhikrishnan, and N. Bolan, Environmental applications of chitosan and its derivatives, in Reviews of Environmental Contamination and Toxicology Volume 233. 2015, Springer. p. 1-43.

45. Hirano, S., K. Hirochi, K.-i. Hayashi, T. Mikami, and H. Tachibana, Cosmetic and pharmaceutical uses of chitin and chitosan, in Cosmetic and Pharmaceutical Applications of Polymers. 1991, Springer. p. 95-104.

46. Cheng, G., P. Varanasi, C. Li, H. Liu, Y.B. Melnichenko, B.A. Simmons, M.S. Kent, and S. Singh, Transition of cellulose crystalline structure and surface morphology of biomass as a function of ionic liquid pretreatment and its relation to enzymatic hydrolysis. Biomacromolecules, 2011. 12(4): p. 933-941.

47. Sun, W., Processing and Microfabrication of Self-Assembled Chitin Nanofibers and Composites. 2014, M.S Thesis University of Washington. p. 5-32.

48. Pang, J., X. Liu, X. Zhang, Y. Wu, and R. Sun, Fabrication of cellulose film with enhanced mechanical properties in ionic liquid 1-allyl-3-methylimidaxolium chloride (AmimCl). Materials, 2013. 6(4): p. 1270-1284.

49. Fernandes, L.L., C.X. Resende, D.S. Tavares, G.A. Soares, L.O. Castro, and J.M. Granjeiro, Cytocompatibility of chitosan and collagen-chitosan scaffolds for tissue engineering. Polimeros, 2011. 21(1): p. 1-6.

50. Hu, X., D. Kaplan, and P. Cebe, Determining beta-sheet crystallinity in fibrous proteins by thermal analysis and infrared spectroscopy. Macromolecules, 2006. 39(18): p. 6161-6170.

51. Kumirska, J., M. Czerwicka, Z. Kaczyński, A. Bychowska, K. Brzozowski, J. Thöming, and P. Stepnowski, Application of spectroscopic methods for structural analysis of chitin and chitosan. Marine Drugs, 2010. 8(5): p. 1567-1636.

52. Kathirgamanathan, K., W.J. Grigsby, J. Al-Hakkak, and N.R. Edmonds, Two-Dimensional FTIR as a Tool to Study the Chemical Interactions within Cellulose-Ionic Liquid Solutions. International Journal of Polymer Science, 2015. 2015: p. 1-9.

53. Youngs, T., C. Hardacre, and J. Holbrey, Glucose solvation by the ionic liquid 1, 3-dimethylimidazolium chloride: A simulation study. The Journal of Physical Chemistry B, 2007. 111(49): p. 13765-13774.

54. Teimouri, A. and M. Azadi, Preparation and characterization of novel chitosan/nanodiopside/nanohydroxyapatite composite scaffolds for tissue engineering applications. International Journal of Polymeric Materials and Polymeric Biomaterials, 2016. 65(18): p. 917-927.

55. Köll, P., G. Borchers, and J. Metzger, Thermal degradation of chitin and cellulose. Journal of Analytical and Applied Pyrolysis, 1991. 19: p. 119-129.

56. Hu, X., K. Shmelev, L. Sun, E.-S. Gil, S.-H. Park, P. Cebe, and D.L. Kaplan, Regulation of silk material structure by temperature-controlled water vapor annealing. Biomacromolecules, 2011. 12(5): p. 1686-1696.

57. Kittur, F., K.H. Prashanth, K.U. Sankar, and R. Tharanathan, Characterization of chitin, chitosan and their carboxymethyl derivatives by differential scanning calorimetry. Carbohydrate Polymers, 2002. 49(2): p. 185-193.

58. Oh, D.X., S. Shin, C. Lim, and D.S. Hwang, Dopamine-mediated sclerotization of regenerated chitin in ionic liquid. Materials, 2013. 6(9): p. 3826-3839.

59. Jayakumar, R., K.P. Chennazhi, S. Srinivasan, S.V. Nair, T. Furuike, and H. Tamura, Chitin scaffolds in tissue engineering. International Journal of Molecular Sciences, 2011. 12(3): p. 1876-1887.

60. Lefèvre, T., M.-E. Rousseau, and M. Pézolet, Protein secondary structure and orientation in silk as revealed by Raman spectromicroscopy. Biophysical Journal, 2007. 92(8): p. 2885-2895.

61. Zhang, C., X. Chen, and Z. Shao, Sol–Gel Transition of Regenerated Silk Fibroins in Ionic Liquid/Water Mixtures. ACS Biomaterials Science & Engineering, 2015. 2(1): p. 12-18.

62. Jaworska, M.M., T. Kozlecki, and A. Gorak, Review of the application of ionic liquids as solvents for chitin. Journal of Polymer Engineering, 2012. 32(2): p. 67-69.

63. Brugnerotto, J., J. Lizardi, F. Goycoolea, W. Argüelles-Monal, J. Desbrieres, and M. Rinaudo, An infrared investigation in relation with chitin and chitosan characterization. Polymer, 2001. 42(8): p. 3569-3580.

64. Gallego, R., J.F. Arteaga, C. Valencia, and J.M. Franco, Isocyanate-functionalized chitin and chitosan as gelling agents of castor oil. Molecules, 2013. 18(6): p. 6532-6549.

65. Wendler, F., F. Meister, D. Wawro, E. Wesolowska, D. Ciechanska, B. Saake, J. Puls, N. Le Moigne, and P. Navard, Polysaccharide blend fibres formed from NaOH, N-methylmorpholine-N-oxide and 1-ethyl-3-methylimidazolium acetate. Fibres and Textiles in Eastern Europe, 2010. 18(2): p. 21-30.

66. Silva, S.S., A.R.C. Duarte, A.P. Carvalho, J.F. Mano, and R.L. Reis, Green processing of porous chitin structures for biomedical applications combining ionic liquids and supercritical fluid technology. Acta Biomaterialia, 2011. 7(3): p. 1166-1172.

67. Zhao, D., Y. Liao, and Z. Zhang, Toxicity of ionic liquids. Clean–Soil, Air, Water, 2007. 35(1): p. 42-48.

68. Sabudin, S., M. Derman, I. Zainol, and K. Noorsal, In vitro cytotoxicity and cell seeding studies of a chitosan-silver composite for potential wound management applications. Journal of Engineering Science, 2012. 8: p. 29-37.

69. Peter, M., N. Ganesh, N. Selvamurugan, S. Nair, T. Furuike, H. Tamura, and R. Jayakumar, Preparation and characterization of chitosan–gelatin/nanohydroxyapatite composite scaffolds for tissue engineering applications. Carbohydrate Polymers, 2010. 80(3): p. 687-694.

70. Zdarta, J., Ł. Klapiszewski, M. Wysokowski, M. Norman, A. Kołodziejczak-Radzimska, D. Moszyński, H. Ehrlich, H. Maciejewski, A.L. Stelling, and T. Jesionowski, Chitin-lignin material as a novel matrix for enzyme immobilization. Marine Drugs, 2015. 13(4): p. 2424-2446.